

**Silver(I) Complexes with 1'-(Diphenylphosphino)-1-cyanoferrocene:
The Art of Improvisation in Coordination**

Karel Škoch, Filip Uhlík, Ivana Císařová and Petr Štěpnička*

Supporting Information

Contents

Experimental details	S-2
IR spectra of 3' and $[(\mu(\text{P},\text{N})\text{-}\mathbf{1})\{\text{CuCl}(\mathbf{1}\text{-}\kappa\text{P})\}]_2$	S-9
X-ray crystallography	S-10
Additional structural drawings and structural data	S-17
DFT computations	S-32
Additional plots of the electron density and its Laplacian	S-33
References	S-37

Materials and Methods. All manipulations were performed under an argon atmosphere and with an exclusion of the direct daylight. Compound **1** was prepared as previously reported.¹ AgCl was precipitated freshly before use and dried under vacuum. Ag₂[SiF₆] was obtained by dissolving freshly prepared Ag₂O (in a slight excess) in 34% aqueous H₂[SiF₆] (Sigma-Aldrich) and evaporation of the filtered reaction mixture. The IR spectrum of thus obtained material was in agreement with the literature.² [Ag(MeCN)₂][B{C₆H₃(CF₃)_{2-3,5}}]₄ was synthesized as described elsewhere.³ Dichloromethane was dried and deoxygenated with an in-house PureSolv MD5 solvent purification system (Innovative Technology). CHCl₃, CDCl₃ and ethyl acetate were dried over calcium hydride. Other chemicals (Alfa-Aesar and Sigma-Aldrich) and reagent-grade solvents (Lachner, Czech Republic) were used as received. NMR spectra were recorded at 25 °C with a Varian UNITY Inova 400 spectrometer operating at 399.95, 376.29 and 161.90 MHz for ¹H, ¹⁹F and ³¹P, respectively. Chemical shifts (δ in ppm) are given relative to internal SiMe₄ (¹H NMR), external neat CFC₃ (¹⁹F NMR) or to external 85% aqueous H₃PO₄ (³¹P NMR), all set to 0 ppm. In addition to the usual notation of signal multiplicity, vt and vq are used to denote virtual triplets and quartets arising from the AA'BB' (C₅H₄CN) and AA'BB'X (C₅H₄PPh₂; A, B = ¹H, X = ³¹P) spin systems constituted by the protons at the ferrocene cyclopentadienyl rings (fc = ferrocene-1,1'-diyl). IR spectra⁴ were measured on an FTIR Nicolet 760 instrument in the range 400-4000 cm⁻¹. Electrospray ionization mass spectra (ESI MS) were obtained on a Bruker Esquire 3000 spectrometer for samples dissolved in HPLC-grade methanol. Elemental analyses were determined by the standard combustion method using a Perkin-Elmer CHNO/S PE 2400 Series II analyzer. If present, the amount of clathrated solvents was confirmed by NMR analysis.

Safety note. Caution. Although we have not encountered any problems, it should be noted that transition metal complexes with organic ligands and perchlorate anions are potentially explosive and should be handled only in small quantities and with care.

Synthesis of [Ag(1-κP)(μ₃-Cl)]₄ (2**).** A mixture of ligand **1** (20 mg, 51 μmol) and silver(I) chloride (7.3 mg, 51 μmol) was stirred in CDCl₃ (2 mL) for 90 min. The still slightly turbid reaction mixture was filtered through a PTFE syringe filter (pore size 0.45 μm) and evaporated under vacuum, leaving a residue, which was immediately crystallized from acetone-hexane (3 + 9 mL). The separated orange crystals were filtered off, washed with pentane and dried under vacuum. Yield of **2**: 23 mg (78%).

^1H NMR (*in situ*, CDCl_3): δ 4.42 (vt, $J' = 1.8$ Hz, 2 H, fc), 4.54 (br s, 2 H, fc), 4.57 (vt, $J' = 1.7$ Hz, 2 H, fc), 4.65 (br s, 2 H, fc), 7.29-7.40 (m, 6 H, PPh_2), 7.57-7.65 (m, 4 H, PPh_2). $^{31}\text{P}\{^1\text{H}\}$ NMR (*in situ*, CDCl_3): δ -1.4 (d, $^1J_{\text{AgP}} = 604$ Hz). ESI+ MS: m/z 502 ($[\text{Ag}(\mathbf{1})]^+$), 645 ($[\text{Ag}_2(\mathbf{1})\text{Cl}]^+$), 897 ($[\text{Ag}(\mathbf{1})_2]^+$). IR (Nujol, cm^{-1}): ν_{max} 3051 w, $\nu_{\text{C}\equiv\text{N}}$ 2227 s, 1710 w, 1232 m, 1169 m, 1098 s, 1033 m, 998 w, 913 w, 836 m, 745 s, 696 s, 632 w, 556 w, 532 m, 512 m, 477 m, 459 m, 434 w. Anal. calc. for $\text{C}_{23}\text{H}_{18}\text{NAgClFeP}$ (538.5): C 51.29, H 3.37, N 2.60%. Found: C 51.24, H 3.41, N 2.40%.

Synthesis of $[\text{Ag}(\mathbf{1}-\kappa\text{P})_2(\mu\text{-Cl})]_2$ (3**).** The same reaction was repeated at the Ag:**1** ratio 1:2, starting with **1** (20 mg, 51 μmol) and AgCl (3.7 mg, 26 μmol) in 2 mL of CDCl_3 . Work-up as above and crystallization from dichloromethane (2 mL) and methyl *t*-butyl ether/hexane (2 + 8 mL) afforded two types of crystals: fine yellow needles (minor) and dark orange prisms, which were separated on the basis of different sedimentation properties (*i.e.*, by improvised flotation).

The dominating orange prisms were identified as dimer **3** (17 mg, 70%). IR (DRIFTS, neat, cm^{-1}): ν_{max} 3128 m, 3097 m, 3051 m, 3014 m, $\nu_{\text{C}\equiv\text{N}}$ 2224 s, 1974 w, 1917 w, 1817 w, 1683 w, 1587 m, 1571 m, 1481 s, 1436 s, 1387 m, 1371 m, 1310 s, 1259 w, 1233 s, 1194 w, 1167 s, 1098 s, 1051 m, 1038 m, 1028 s, 997 m, 911 m, 838 s, 752 s, 704 s, 633 m, 557 s, 530 s, 514 s, 494 s, 429 m. Anal. calc. for $\text{C}_{46}\text{H}_{36}\text{N}_2\text{AgClFe}_2\text{P}_2$ (933.7): C 59.17, H 3.89, N 3.00%. Found: C 58.96, H 3.73, N 2.90%.

The minor product (**3'**): yellow needles, 4 mg (28%). IR (DRIFTS, neat, cm^{-1}): ν_{max} 3107 w, 3073 m, $\nu_{\text{C}\equiv\text{N}}$ 2228 s, 1480 m, 1437 s, 1388 w, 1312 w, 1231 m, 1171 m, 1098 m, 1030 m, 912 w, 838 m, 748 s, 696 vs, 556 w, 534 m, 512 s, 491 s, 478 s, 458 s, 438 w.

The reaction performed at the Ag:**1** ratio of 1:3 (**1**: 20 mg, 51 μmol ; AgCl: 2.4 mg, 17 μmol) and subsequent crystallization from acetone-hexane (2 + 10 mL) afforded **3** as the sole crystalline product (12 mg, 75%).

Synthesis of $[\text{Ag}(\mathbf{1}-\kappa\text{P})(\mu_3\text{-Br})]_4$ (4**).** Ligand **1** (20 mg, 51 μmol) and AgBr (9.5 mg, 51 μmol) were reacted in CDCl_3 (2 mL) for 60 min. Filtration of the resultant cloudy solution, evaporation and crystallization from reagent-grade ethyl acetate-hexane (2 + 20 mL) furnished **4**· H_2O as orange needles (26 mg, 85%).

^1H NMR (*in situ*, CDCl_3): δ 4.43 (br s, 2 H, fc), 4.58 (br s, 6 H, fc), 7.28-7.39 (m, 6 H, PPh_2), 7.56-7.64 (m, 4 H, PPh_2). $^{31}\text{P}\{^1\text{H}\}$ NMR (*in situ*, CDCl_3): very broad and composite signal

centered at $\delta_{\text{P}} - 8$ ppm. ESI+ MS: m/z 434 ($[\mathbf{1} + \text{K}]^+$), 502 ($[\text{Ag}(\mathbf{1})]^+$), 606 ($[\text{Ag}(\mathbf{1})\text{Br} + \text{Na}]^+$). IR (Nujol, cm^{-1}): ν_{max} 3600 br w, 3524 br w, 3086 w, 3069 w, 3054 w, $\nu_{\text{C}\equiv\text{N}}$ 2225 s, 1311 w, 1232 m, 1209 w, 1198 w, 1170 m, 1097 m, 1070 w, 1061 w, 1031 s, 998 w, 913 m, 837 m composite, 754 m, 743 s, 694 s, 631 w, 555 w, 531 m, 509 s, 492 m, 477 s, 457 s, 431 w. Anal. calc. for $\text{C}_{23}\text{H}_{18}\text{NAgBrFeP}\cdot\text{H}_2\text{O}$ (601.0): C 45.96, H 3.35, N 2.33%. Found: C 45.76, H 2.95, N 2.10%.

Synthesis of $[\text{Ag}(\mathbf{1}-\kappa\text{P})(\mu_3\text{-I})_4]$ (5**).** Reaction between **1** (20 mg, 51 μmol) and AgI (12 mg, 51 μmol) and subsequent crystallization as described above for **4** provided complex **5** as orange, plate-like crystals (17 mg, 54%).

^1H NMR (*in situ*, CDCl_3): δ 4.44 (vt, $J' = 1.9$ Hz, 2 H, fc), 4.49 (vt, $J' = 1.9$ Hz, 2 H, fc), 4.59 (vt, $J' = 1.8$ Hz, 2 H, fc), 4.62 (vq, $J' = 1.8$ Hz, 2 H, fc), 7.28-7.34 (m, 4 H, PPh_2), 7.36-7.41 (m, 2 H, PPh_2), 7.55-7.62 (m, 4 H, PPh_2). $^{31}\text{P}\{^1\text{H}\}$ NMR (*in situ*, CDCl_3): δ -14.6 (d, $^1J_{\text{AgP}} = 504$ Hz). ESI+ MS: m/z 418 ($[\mathbf{1} + \text{Na}]^+$), 502 ($[\text{Ag}(\mathbf{1})]^+$), 652 ($[\text{Ag}(\mathbf{1})\text{I} + \text{Na}]^+$). IR (Nujol, cm^{-1}): ν_{max} 3103 m, 3089 m, 3073 m, 3049 m, $\nu_{\text{C}\equiv\text{N}}$ 2226 s, 1736 w, 1683 w, 1585 w, 1570 w, 1309 m, 1232 m, 1196 m, 1168 s, 1099 s, 1070 w, 1060 w, 1029 s, 998 w, 970 w, 914 m, 890 w, 837 s, 745 s, 695 s, 632 w, 556 m, 531 s, 510 s, 477 s, 456 s, 432 m. Anal. calc. for $\text{C}_{23}\text{H}_{18}\text{NAgFeIP}$ (630.0): C 43.85, H 2.88, N 2.22%. Found: C 43.59, H 2.82, N 1.93%.

Synthesis of $[(\mathbf{1}-\kappa\text{P})_2\text{Ag}(\text{NC})\text{Ag}(\text{CN})]_n$ (6**).** Silver(I) cyanide (7 mg, 51 μmol) and **1** (20 mg, 51 μmol) were dissolved in CDCl_3 (2 mL) by stirring for 60 min. The reaction mixture was evaporated under vacuum and the resulting glassy residue was dissolved in acetone (2 mL). The solution was filtered and layered with hexane (10 mL). Slow crystallization furnished **6** as orange needles (24 mg, 89%). Similar reaction at Ag:**1** molar ratio of 1:2 (i.e., with 3.5 mg (25 μmol) of AgCN) and crystallization led to the same compound.

^1H NMR (*in situ*, CDCl_3): δ 4.40 (vq, $J' = 1.9$ Hz, 2 H, fc), 4.42 (vt, $J' = 1.9$ Hz, 2 H, fc), 4.51 (vt, $J' = 2.1$ Hz, 2 H, fc), 4.64 (vt, $J' = 1.8$ Hz, 2 H, fc), 7.33-7.47 (m, 10 H, PPh_2). $^{31}\text{P}\{^1\text{H}\}$ NMR (*in situ*, CDCl_3): δ -0.6 (br s). ESI+ MS: m/z 502 ($[\text{Ag}(\mathbf{1})]^+$), 551 ($[\text{Ag}(\mathbf{1})\text{CN} + \text{Na}]^+$). IR (Nujol, cm^{-1}): ν_{max} 3105 w, 3054 w, $\nu_{\text{C}\equiv\text{N}}$ 2227 s, $\nu_{\text{C}\equiv\text{N}}$ 2149 m, 1309 w, 1231 w, 1196 w, 1167 m, 1096 m, 1071 w, 1058 w, 1030 m, 999 m, 913 m, ca. 830 br m, 746 s, 697 s, 631 w, 556 w, 530 m, 511 m, 491 m, 475 s, 458 s, 434 m. Anal. calc. for $\text{C}_{24}\text{H}_{18}\text{N}_2\text{AgFeP}$ (529.1): C 54.48, H 3.43, N 5.30%. Found: C 54.40, H 3.43, N 4.91%.

Synthesis of [Ag(μ_3 -SCN-*S,S,N*)(1- κ P)]₄ (7**).** A mixture of ligand **1** (20 mg, 51 μ mol) and AgSCN (8.5 mg, 51 μ mol) in CDCl₃ (2 mL) was stirred for 20 h. The resulting turbid reaction mixture was filtered and evaporated to afford an orange residue, which was immediately dissolved in ethyl acetate (3 mL). Layering with hexane (9 mL) and crystallization by liquid-phase diffusion gave **7** as orange crystalline solid. Yield: 22 mg (78%).

¹H NMR (*in situ*, CDCl₃): δ 4.41 (d vt, J' = 2.8 Hz, 1.8 Hz, 2 H, fc), 4.55 (vt, J' = 1.8 Hz, 2 H, fc), 4.60 (vt, J' = 1.8 Hz, 2 H, fc), 4.65 (vt, J' = 1.9 Hz, 2 H, fc), 7.22-7.28 (m, 4 H, PPh₂), 7.31-7.41 (m, 6 H, PPh₂). ³¹P{¹H} NMR (*in situ*, CDCl₃): very broad doublet centered at δ_P ca. -1. ESI+ MS: m/z 502 ([Ag(**1**)⁺], 897 ([Ag(**1**)₂]⁺). IR (Nujol, cm⁻¹): ν_{\max} 3101 w, 3089 w, 3054 w, $\nu_{C\equiv N}$ 2237 s, $\nu_{C\equiv N}$ 2227 m, ν_{SCN} 2122 m, ν_{SCN} 2094 vs, 1310 w, 1269 w, 1236 w, 1195 w, 1168 m, 1096 m, 1029 m, 998 w, 916 w, 840 m, 827 m, 746 s, 697 s, 631 w, 557 w, 531 m, 509 m, 491 s, 460 s, 439 m. Anal. calc. for C₂₄H₁₈N₂AgFePS (561.1): C 51.37, H 3.23, N 4.99%. Found: C 51.43, H 3.21, N 4.72%.

Preparation of [Ag(1- κ P)₂(μ -SCN-*S,S,N*)]₂ (8**).** The synthesis of **8** was performed similarly, using 4.5 mg (25 μ mol) of AgSCN. The crude product resulting after evaporation was crystallized from chloroform-hexane (1 + 10 mL), yielding **8** as orange crystals (23 mg, 95%). ¹H NMR (*in situ*, CDCl₃): δ 4.38 (vq, J' = 2.1 Hz, 2 H, fc), 4.47-4.49 (m, 4 H, fc), 4.59 (vt, J' = 1.9 Hz, 2 H, fc), 7.30-7.36 (m, 4 H, PPh₂), 7.37-7.44 (m, 6 H, PPh₂). ³¹P{¹H} NMR (*in situ*, CDCl₃): δ -2.6 (br s). ESI+ MS: m/z 502 ([Ag(**1**)⁺], 669 ([Ag₂(**1**)SCN]⁺), 897 ([Ag(**1**)₂]⁺). IR (Nujol, cm⁻¹): ν_{\max} 3124 w, 3110 m, 3095 w, 3056 m, 3042 w, $\nu_{C\equiv N}$ 2239 m, $\nu_{C\equiv N}$ 2226 s, ν_{SCN} 2098 s, 1737 w, 1583 w, 1309 m, 1232 m, 1192 m, 1166 s, 1098 s, 1069 w, 1058 w, 1028 s, 997 w, 972 w, 913 w, 890 w, 840 s, 827 m, 752 s, 744 s, 697 s, 634 w, 557 m, 529 m, 511 s, 482 s, 469 m, 459 s, 437 w. Anal. calc. for C₄₇H₃₆N₃AgFe₂P₂S (956.4): C 59.02, H 3.79, N 4.39%. Found: C 59.00, H 3.67, N 4.40%.

Reactions of **1 with AgF.** Silver(I) fluoride weighed on a glass culet was dropped into a solution of ligand **1** in dry ethyl acetate (2 mL) and the resulting mixture was stirred for 24 h, whereupon the solid halide dissolved. Subsequent filtration, layering with hexane (10 mL) and crystallization by liquid phase diffusion afforded orange crystals, which were subjected to X-ray diffraction analysis. The product of the reaction performed at the 1:1 silver-to-**1** molar ratio (6.5 mg of AgF and 20 mg of **1**) was identified as a co-crystal consisted of [Ag(μ -HF₂)(1- κ P)₂]₂ (**9**) and dimer **3**. Unfortunately, poor quality of the available data and disorder

precluded any further refinement. The analogous reaction at the 1:2 AgF-to-**1** molar ratio (3.2 mg of AgF and 20 mg of **1**) afforded a tiny amount (*very few crystals*) of compound **10**. Further attempts at obtaining crystalline products by crystallization from different solvents (methanol and acetone) only led to the formation of silver mirror and intractable dark precipitates.

Synthesis of $(\mu\text{-SiF}_6)[\text{Ag}(\mathbf{1}\text{-}\kappa\text{P})_2]_2$ (10**).** Silver(I) hexafluorosilicate (4.5 mg, 12.5 μmol) and nitrile **1** (20 mg, 51 μmol) were mixed in CHCl_3 (2 mL) and the resulting mixture was stirred for 2 h. Then, the volume of the reaction mixture was reduced to the half and the residue was filtered through a PTFE syringe filter (0.45 μm). The product was crystallized by addition of acetone (1 mL) and layering with hexane (10 mL) to afford solvate $\mathbf{10}\cdot\frac{1}{2}\text{CHCl}_3\cdot\frac{1}{2}\text{Me}_2\text{CO}$ as orange crystals. Yield: 18 mg (71%).

^1H NMR (*in situ*, CDCl_3): δ 4.45 (br s, 4 H, fc), 4.51 (br s, 2 H, fc), 4.57 (br s, 2 H, fc), 7.26-7.32 (m, 4 H, PPh_2), 7.33-7.39 (m, 2 H, PPh_2), 4.42-4.47 (m, 4 H, PPh_2). $^{19}\text{F}\{^1\text{H}\}$ NMR (*in situ*, CDCl_3): δ -131.04 (s with ^{29}Si satellites, $^1J_{\text{SiF}} = 115$ Hz). $^{31}\text{P}\{^1\text{H}\}$ NMR (*in situ*, CDCl_3): very broad signal centred at δ_{P} ca. -2. ESI+ MS: m/z 502 ($[\text{Ag}(\mathbf{1})]^+$), 897 ($[\text{Ag}(\mathbf{1})_2]^+$). IR (Nujol, cm^{-1}): ν_{max} 3104 m, 3056 m, $\nu_{\text{C}\equiv\text{N}}$ 2223 s, $\nu_{\text{C}=\text{O}}$ 1705 s (acetone), 1586 w, 1571 w, 1310 w, 1226 m, 1170 m, 1100 m, 1070 w, 1034 m, 999 w, 913 w, 842 m composite, $\nu_3([\text{SiF}_6]^{2-})$ 749 s composite, 694 s composite, 557 w, 532 m, 513 s, 477 s, 460 s, 433 m. Anal. calc. for $\text{C}_{92}\text{H}_{72}\text{N}_4\text{Ag}_2\text{F}_6\text{Fe}_4\text{P}_4\text{Si}\cdot\frac{1}{2}\text{CHCl}_3\cdot\frac{1}{2}\text{Me}_2\text{CO}$ (2027.3): C 55.68, H 3.75, N 2.76%. Found C 55.37, H 3.79, N 2.48%.

Synthesis of $[\text{Ag}(\mu\text{-}\mathbf{1})]_2(\text{ClO}_4)_2$ (11**).** Ligand **1** (20 mg, 51 μmol) and silver(I) perchlorate (10.5 mg, 51 μmol) were stirred in 2 ml of CH_2Cl_2 for 60 min, during which time an orange precipitate separated. The reaction mixture was evaporated and the residue was dissolved in a mixture of acetone (2 mL) and acetonitrile (0.1 mL). The solution was filtered through a PTFE syringe filter (pore size: 0.45 μm) and layered with hexane (10 mL). Crystallization by liquid-phase diffusion furnished orange crystals, which were isolated by suction and dried under vacuum. Yield of **11**: 21 mg (68%). Reaction at the Ag:**1** ratio of 1:2 afforded an identical product.

ESI+ MS: m/z 502 ($[\text{Ag}(\mathbf{1})]^+$). IR (Nujol, cm^{-1}): ν_{max} 3120 w, 3074 w, 3047 w, $\nu_{\text{C}\equiv\text{N}}$ 2283 m, $\nu_{\text{C}\equiv\text{N}}$ 2272 s, 1711 w, 1586 w, 1311 w, 1242 w, 1172 m, $\nu_3([\text{ClO}_4]^-)$ ca. 1125-1025 s composite, 998 w, 918 w, 897 w, 855 w, 824 s, 752 s, 745 s, 702 s, 694 s, 641 w, $\nu_4([\text{ClO}_4]^-)$

624 s, 588 w, 537 m, 522 m, 513 m, 486 s, 470 s, 460 s, 434 m. Anal. calc. for $C_{23}H_{18}NAgClFeO_4P$ (602.5): C 45.85, H 3.01, N 2.33%. Found: C 46.15, H 3.39, N 2.52%. NMR spectra could not be recorded for solubility reasons.

Synthesis of $[Ag(\mu-1)]_2[BF_4]_2$ (12**).** Ligand **1** (20 mg, 51 μ mol) and $Ag[BF_4]$ (10 mg, 51 μ mol) were reacted in $CDCl_3$ (2 mL) for 60 min, whereupon the clear solution formed initially deposited some orange precipitate. Acetonitrile (0.1 mL) was added to dissolve the separated solid and the resultant solution was filtered and crystallized by addition of hexane (10 mL). The orange-red crystals that separated after few days were isolated by suction and dried under vacuum. Yield of **12** $\cdot 0.1CHCl_3$: 23 mg (76%).

1H NMR (*in situ*, $CDCl_3$): δ 4.42 (vt, $J' = 1.9$ Hz, 2 H, fc), 4.44 (br vq, 2 H, fc), 4.54 (vt, $J' = 1.9$ Hz, 2 H, fc), 4.65 (vt, $J' = 1.8$ Hz, 2 H, fc), 7.35-7.49 (m, 10 H, PPh_2). $^{31}P\{^1H\}$ NMR (*in situ*, $CDCl_3$): δ -3.4 (br s). ESI+ MS: m/z 502 ($[Ag(1)]^+$), 897 ($[Ag(1)_2]^+$). IR (Nujol, cm^{-1}): ν_{max} 3127 w, 3089 w, 3075 w, 3048 w, $\nu_{C\equiv N}$ 2285 s, $\nu_{C\equiv N}$ 2275 s, 1586 w, 1311 w, 1283 w, 1245 w, 1188 w, 1171 m, $\nu_3([BF_4]^-)$ ca. 1100-995 s composite, 918 m, 899 w, 879 w, 826 m, 754 m, 746 m, 641 w, 590 w, 538 m, 523 m, 513 m, 487 m, 470 m, 462 m, 435 m. Anal. calc. for $C_{23}H_{18}NAgBF_4FeP\cdot 0.1CHCl_3$ (601.8): C 46.10, H 3.03, N 2.33%. Found: C 46.34, H 2.97, N 2.16%.

Isolation of $[Ag(\mu-1)(AcOEt-\kappa O)]_2[SbF_6]_2$ (13**).** In an analogous experiment, ligand **1** (20 mg, 51 μ mol) and $Ag[SbF_6]$ (17.5 mg, 51 μ mol) were reacted in 2 mL of $CDCl_3$. Evaporation and crystallization from ethyl acetate-hexane (3 + 10 mL) yielded **13** as fine orange prisms (31 mg, 75%).

1H NMR (*in situ*, $CDCl_3$): δ 4.46 (vt, $J' = 1.82$ Hz, 2 H, CH of fc), 4.49 (br s, 2 H, CH of fc), 4.61 (br s, 2 H, CH of fc), 4.74 (vt, $J' = 1.82$ Hz, 2 H, CH of fc), 7.40-7.55 (m, 10 H, PPh_2). $^{31}P\{^1H\}$ NMR (*in situ*, $CDCl_3$): δ -1.7 (d, $^1J_{AgP} = 535$ Hz). ESI+ MS: m/z 502 ($[Ag(1)]^+$). IR (Nujol, cm^{-1}): ν_{max} 3123 w, 3057 w, $\nu_{C\equiv N}$ 2280 m, $\nu_{C\equiv N}$ 2267 s, $\nu_{C\equiv N}$ 2255 m, $\nu_{C=O}$ 1703 s, 1300 w, 1260 s, 1241 m, 1200 w, 1173 m, 1100 m, 1036 m, 998 w, 917 w, 848 w, 836 w, 827 w, 748 s, 698 s, $\nu_3([SbF_6]^-)$ 661 vs, 540 w, 519 w, 511 w, 488 m, 473 m, 460 m, 435 w. Anal. calc. for $C_{54}H_{52}N_2Ag_2F_{12}Fe_2O_4P_2Sb_2$ (826.9): C 39.21, H 3.17, N 1.69%. Found: C 39.50, H 2.95, N 2.04%. Attempted reactions performed at the $Ag[SbF_6]:1$ ratio of 1:2 did not yield any defined crystalline product.

[Ag(μ -1)]₂[B{C₆H₃(CF₃)₂-3,5}]₄ (14**). Ligand **1** (20 mg, 51 μ mol) and [Ag(MeCN)₂][B{C₆H₃(CF₃)₂-3,5}]₄ (53 mg, 51 μ mol) were dissolved in chloroform (2 mL). The resultant solution was stirred in the dark for 60 min and then filtered through a PTFE syringe filter (pore size 0.45 μ m). The filtrate was layered with hexane (10 mL) and the mixture was set aside for crystallization. Orange crystals that separated during several days (along with some amorphous, brown gummy precipitate) were isolated by suction on a coarse frit, washed with pentane and dried under vacuum. Yield of **14**: 57 mg (82%), orange prismatic crystals.**

¹H NMR (acetone-d₆): δ 4.45 (vt, J' = 2.0 Hz, 2 H, fc), 4.65 (br vt J' = 1.8 Hz, 2 H, fc), 4.78 (br vt J' = 1.8 Hz, 2 H, fc), 4.88 (vt, J' = 2.0 Hz, 2 H, fc), 7.54-7.68 (m, 14 H, PPh₂ and H-4 of C₆H₃), 7.79 (m, 8 H, H-2,6 of C₆H₃). ¹⁹F{¹H} NMR (acetone-d₆): δ -62.5 (s). ³¹P{¹H} NMR (acetone-d₆): δ 5.5 (d, ¹J_{AgP} = 765 Hz). ESI+ MS: m/z 502 ([Ag(**1**)]⁺), 897 ([Ag(**1**)₂]⁺). ESI- MS: m/z 863 ([B{C₆H₃(CF₃)₂}₄]⁻). Note: Unlike the previous cases, the NMR and MS spectra were recorded for a *crystallized* product. IR (Nujol, cm⁻¹): ν_{\max} 3099 w, 3064 w, $\nu_{\text{C}\equiv\text{N}}$ 2282 w, $\nu_{\text{C}\equiv\text{N}}$ 2258 s, 1611 m, 1356 s, 1278 s, ca. 1180-1115 s composite, 1062 w, 1035 w, 1000 w, 899 m, 887 s, 838 s, 747 s, 715 s, 694 m, 682 s, 670 s, 634 w, 593 w, 541 m, 518 m, 512 m, 490 m, 472 m, 463 m, 448 w, 440 w. Anal. Calc. for C₅₅H₃₀NAgBF₂₄FeP (1366.3): C 48.35, H 2.21, N 1.03%. Found C 48.03, H 2.19, N 0.90%.

Preparation [Ag(1- κ P)(μ -1)]_n[BF₄]_n (15**). Ligand **1** (20 mg, 51 μ mol) and Ag[BF₄] (5 mg, 25 μ mol) were reacted in 2 ml of CDCl₃ for 60 min. The resulting mixture was filtered through a PTFE syringe filter and the filtrate was partially evaporated under vacuum (to ca. 0.1 mL). The residue was mixed with ethyl acetate (2 mL), the solution was carefully layered with hexane (10 mL) and allowed to crystallize at 4 °C. The crystalline solid was filtered off, washed with pentane and dried under vacuum to afford **15**·AcOEt (22 mg, 80%). A similar reaction at the Ag:**1** ratio of 1:3 (Ag[BF₄]: 3.5 mg, 17 μ mol) gave the same product.**

¹H NMR (*in situ*, CDCl₃): δ 4.46 (vt, J' = 1.9 Hz, 2 H, fc), 4.52 (br vt, 2 H, fc), 4.57 (vt, J' = 2 Hz, 2 H, fc), 4.68 (vt, J' = 1.9 Hz, 2 H, fc), 7.35-7.51 (m, 10 H, PPh₂). ³¹P{¹H} NMR (*in situ*, CDCl₃): δ -1.4 (br s). ESI+ MS: m/z 502 ([Ag(**1**)]⁺), 897 ([Ag(**1**)₂]⁺). IR (Nujol, cm⁻¹): ν_{\max} 3124 w, 3053 w, $\nu_{\text{C}\equiv\text{N}}$ 2242 m, $\nu_{\text{C}\equiv\text{N}}$ 2228 m, $\nu_{\text{C}\equiv\text{N}}$ 2214 s, 1712 s, 1309 w, 1236 w, 1196 w, 1169 m, ν_3 ([BF₄]⁻) ca. 1085-1025 s composite, 998 w, 913 w, 746 m, 727 m, 696 s, 629 w, 557 w, 535 w, 511 m, 480 s, 459 s. Anal. calc. for C₄₆H₃₆N₂AgBF₄Fe₂P₂·CHCl₃ (1104.5): C 51.11, H 3.38, N 2.54%. Found: C 51.34, H 3.34, N 2.30% (sample from chloroform-hexane).

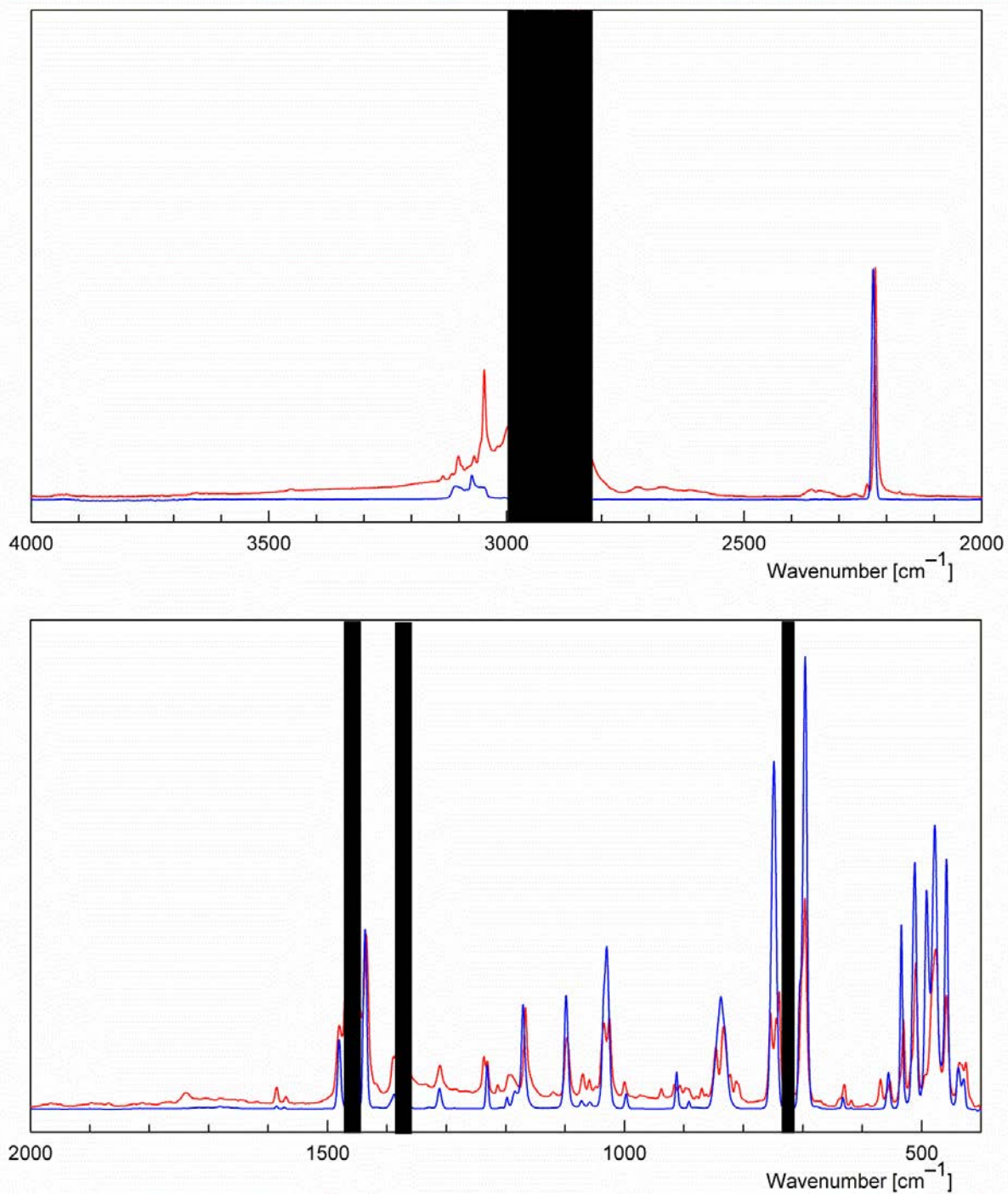


Figure S1. Comparison of the IR spectra recorded for **3'** (red; in diffuse reflectance mode) and for complex $[(\mu(\text{P},\text{N})\text{-1})\{\text{CuCl}(\text{1-}\kappa\text{P})\}]_2$ described previously¹ (blue; conventional transmission mode, Nujol suspension). Nujol absorptions are indicated with black boxes.

X-ray Crystallography

All single crystals used for X-ray diffraction measurements were grown by layering the respective reaction mixture with a less polar solvent and slow crystallization by liquid-phase diffusion. Thus, the crystals of **2**·H₂O were obtained by diffusion of hexane into a solution in reagent-grade acetone containing ca. 2-5% of water while those of **3**·CH₂Cl₂ were isolated from dichloromethane/methyl *tert*-butyl ether-hexane. Crystals of **4**·0.25H₂O and **5**·3AcOEt were obtained from ethyl acetate/hexane. A different solvatomorph, **5**·4CHCl₃, resulted by crystallization of a AgI-**1** mixture (Ag:**1** = 1:2) from chloroform/hexane. The crystals of polymeric **6** were grown from hexane/acetone. Compounds **7**, **8**, **14** and **16** were crystallized from chloroform/hexane while the crystals of **15**·AcOEt, **13**, **17** and **18** were obtained from ethyl acetate/hexane. Complex **10**·½Me₂CO·½CHCl₃ was crystallized from acetone-chloroform/hexane. Compound **11** was crystallized from acetone/hexane with *little* added acetonitrile for solubility reasons. The crystals of complex **12** were obtained similarly but from chloroform-acetonitrile/hexane.

Full-set diffraction data ($\pm h\pm k\pm l$; $\theta_{\max} = 26.0$ or 27.5° , data completeness $\geq 99.8\%$) were collected at 150(2) K with a Bruker Apex II CCD diffractometer equipped with a Cryostream Cooler (Oxford Cryosystems) using graphite-monochromatized MoK α radiation ($\lambda = 0.71073$ Å). The data were corrected for absorption by the methods included in the diffractometer software. The structures were solved by the direct methods (SHELXS97⁵) and refined by full-matrix least-squares routine based on F^2 (SHELXL97⁵ or SHELXL-2014⁶). Unless noted otherwise, the non-hydrogen atoms were refined with anisotropic displacement parameters while the hydrogens (CH_{*n*}) were included in their calculated positions and refined as riding atoms with U_{iso} set to a multiple of U_{eq} of the respective carbon atom. Relevant crystallographic data and structure refinement parameters are given in the Supporting Information, Table S1. Particular details on structure refinement are as follows.

In many cases, the peripheral moieties, typically the C₅H₄CN moieties in compounds with P-monodentate **1**, show partial disorder. This apparently reflects molecular mobility increasing from the compact and rigid core to the periphery. Similarly, solvent molecules in crystalline solvates are often disordered, filling structural voids between bulky complex molecules without interacting with them. For instance, the solvent molecule in the structure of **3**·CH₂Cl₂ is disordered and was modelled over four positions using SIMU restraints. Similarly, one of the solvating ethyl acetate molecules in the structure of **5**·3AcOEt was disordered around an

inversion center and could not be properly modelled. Therefore, its contributions to scattering were removed using the SQUEEZE⁷ routine in PLATON.⁸ In the case of **6**, the solvents of crystallization (acetone and hexane) were heavily disordered in the space left between the polymeric chains and were thus treated analogously. Similar applies to the structures of **7** (ill-defined chloroform solvate) and **10**·½Me₂CO·½CHCl₃, in which also one of the uncoordinated cyano group had to be refined over two positions.

The Ag-coordinate ethyl acetate in **13** is disordered, too, and was refined over two positions (70:30). Because of a close proximity of the contributing orientations, the refinement had to be performed with isotropic displacement factors and some geometry restraints (DFIX). Finally, the [BF₄]⁻ anion in the structure of **15**·AcOEt is disordered and was refined with two positions for three of its fluorine atoms.

PLATON was used for the graphical representation of all structures and geometrical calculations. The numerical values are rounded with respect to their estimated deviations (ESDs) given to one decimal place. Parameters relating to atoms in constrained positions are given without ESDs.

Table S1. Summary of Crystallographic Data and Structure Refinement Parameters.^a

Compound	2 ·H ₂ O	3 ·CH ₂ Cl ₂	4 ·0.25H ₂ O
Formula	C ₉₂ H ₇₄ Ag ₄ Cl ₄ Fe ₄ N ₄ OP ₄	C ₉₃ H ₇₄ Ag ₂ Cl ₄ Fe ₄ N ₄ P ₄	C ₉₂ H _{72.50} Ag ₄ Br ₄ Fe ₄ N ₄ O _{0.25} P ₄
<i>M</i>	2172.11	1952.38	2336.44
Crystal system	triclinic	triclinic	triclinic
Space group	<i>P</i> -1 (no. 2)	<i>P</i> -1 (no. 2)	<i>P</i> -1 (no. 2)
<i>a</i> /Å	14.2409(3)	14.8421(4)	14.4397(3)
<i>b</i> /Å	15.5678(4)	16.8593(5)	15.5216(3)
<i>c</i> /Å	20.0839(4)	18.7465(5)	20.1463(4)
α /°	75.549(1)	64.394(1)	75.795(1)
β /°	83.888(1)	77.568(1)	84.538(1)
γ /°	75.671(1)	74.752(1)	76.015(1)
<i>V</i> /Å ³	4172.8(2)	4053.3(2)	4244.4(2)
<i>Z</i>	2	2	2
μ (Mo K α)/mm ⁻¹	1.848	1.432	3.573
Diffns collected	63467	61134	73683
Independent diffns	19179	18596	19433
Observed ^b diffns	14157	15457	16112
<i>R</i> _{int} ^c /%	4.22	2.59	2.44
No. of parameters	1018	1045	1015
<i>R</i> ^c obsd diffns/%	3.47	3.10	2.29
<i>R</i> , <i>wR</i> ^c all data/%	6.11, 5.79	4.19, 7.40	3.47, 4.31
$\Delta\rho$ /e Å ⁻³	0.50, -0.50	2.05, -1.55	0.75, -0.74
CCDC entry	1470453	1470454	1470455

^a Common details: *T* = 150(2) K. ^b Diffractions with $I > 2\sigma(I)$. ^c Definitions: $R_{\text{int}} = \Sigma |F_o^2 - F_o^2(\text{mean})| / \Sigma F_o^2$, where $F_o^2(\text{mean})$ is the average intensity of symmetry-equivalent diffractions. $R = \Sigma ||F_o| - |F_c|| / \Sigma |F_o|$, $wR = [\Sigma \{w(F_o^2 - F_c^2)^2\} / \Sigma w(F_o^2)^2]^{1/2}$.

Table S1 continued

Compound	5-3AcOEt	5-4CHCl₃	6 (solvated)
Formula	C ₁₀₄ H ₉₆ Ag ₄ Fe ₄ I ₄ N ₄ O ₆ P ₄	C ₉₆ H ₇₆ Ag ₄ Cl ₁₂ Fe ₄ I ₄ N ₄ P ₄	C ₄₈ H ₃₆ Ag ₂ Fe ₂ N ₄ P ₂
<i>M</i>	2784.21	2997.37	1058.19
Crystal system	monoclinic	monoclinic	monoclinic
Space group	<i>C2/c</i> (no. 15)	<i>C2/c</i> (no. 15)	<i>P2₁/n</i> (no. 14)
<i>a</i> /Å	32.5006(6)	33.0189(7)	10.9157(2)
<i>b</i> /Å	12.0171(2)	12.0454(3)	33.0460(6)
<i>c</i> /Å	26.2756(4)	26.0476(6)	13.5246(3)
α /°	90	90	90
β /°	97.249(1)	99.743(1)	90.5317(7)
γ /°	90	90	90
<i>V</i> /Å ³	10180.3(3)	10210.4(4)	4878.4(2)
<i>Z</i>	4	4	4
μ (Mo K α)/mm ⁻¹	2.636	2.935	1.474
Diffns collected	53241	38701	83740
Independent diffns	11715	11720	11219
Observed ^c diffns	10012	10115	10028
<i>R</i> _{int} ^d /%	2.99	2.57	2.39
No. of parameters	561	577	523
<i>R</i> ^d obsd diffns/%	2.97	2.93	2.44
<i>R</i> , <i>wR</i> ^d all data/%	3.76, 7.12	3.74, 6.37	2.97, 5.11
$\Delta\rho$ /e Å ⁻³	1.21, -0.55	0.70, -1.15	0.36, -0.47
CCDC entry	1470456	1470457	1470458

Table S1 continued

Compound	7 (solvated)	8	10 ·1/2CHCl ₃ ·1/2Me ₂ CO
Formula	C ₉₆ H ₆₈ Ag ₄ Fe ₄ N ₈ P ₄ S ₄	C ₉₄ H ₇₂ Ag ₂ Fe ₄ N ₆ P ₄ S ₂	C ₉₂ H ₇₂ Ag ₂ F ₆ Fe ₄ N ₄ P ₄ Si
<i>M</i>	2240.68	1912.72	1938.65
Crystal system	monoclinic	triclinic	monoclinic
Space group	<i>P2/n</i> (no. 13)	<i>P</i> -1 (no. 2)	<i>C2/c</i> (no. 15)
<i>a</i> /Å	13.0647(3)	12.4899(4)	26.7175(8)
<i>b</i> /Å	22.9434(5)	13.2576(4)	14.4939(4)
<i>c</i> /Å	33.3549(9)	13.7984(4)	26.1685(8)
α /°	90	104.055(1)	90
β /°	100.968(1)	111.698(1)	115.336(1)
γ /°	90	96.545(1)	90
<i>V</i> /Å ³	9815.5(4)	2006.1(1)	9158.8(5)
<i>Z</i>	4	1	4
μ (Mo K α)/mm ⁻¹	1.551	1.367	1.176
Diffns collected	58781	28941	38841
Independent diffns	19262	9205	10515
Observed ^c diffns	14831	7941	8928
<i>R</i> _{int} ^d /%	3.55	2.56	3.35
No. of parameters	1082	505	529
<i>R</i> ^d obsd diffns/%	4.68	2.41	4.54
<i>R</i> , <i>wR</i> ^d all data/%	6.14, 13.1	3.18, 5.33	5.55, 9.44
$\Delta\rho$ /e Å ⁻³	1.42, -0.74	0.38, -0.31	0.95, -0.77
CCDC entry	1470459	1470460	1470461

Table S1 continued

Compound	11	12	13
Formula	C ₄₆ H ₃₆ Ag ₂ Cl ₂ Fe ₂ N ₂ O ₈ P ₂	C ₄₆ H ₃₆ Ag ₂ B ₂ F ₈ Fe ₂ N ₂ P ₂	C ₅₄ H ₅₂ Ag ₂ F ₁₂ Fe ₂ N ₂ O ₄ P ₂ Sb ₂
<i>M</i>	1205.05	1179.77	1653.86
Crystal system	monoclinic	monoclinic	monoclinic
Space group	<i>P</i> 2 ₁ / <i>n</i> (no. 14)	<i>P</i> 2 ₁ / <i>n</i> (no. 14)	<i>P</i> 2 ₁ / <i>c</i> (no. 14)
<i>a</i> /Å	8.4383(2)	8.3855(1)	8.4854(2)
<i>b</i> /Å	11.2773(3)	11.1758(2)	14.8856(5)
<i>c</i> /Å	22.8008(5)	22.8296(3)	23.0053(7)
α /°	90	90	90
β /°	97.694(1)	97.128(1)	94.859(1)
γ /°	90	90	90
<i>V</i> /Å ³	2150.22(9)	2122.93(5)	2895.4(2)
<i>Z</i>	2	2	2
μ (Mo K α)/mm ⁻¹	1.816	1.727	2.210
Diffns collected	19998	15408	22910
Independent diffns	4929	4871	6638
Observed ^c diffns	4037	4348	5046
<i>R</i> _{int} ^d /%	3.26	2.08	3.70
No. of parameters	289	289	358
<i>R</i> ^d obsd diffns/%	2.79	2.29	3.47
<i>R</i> , <i>wR</i> ^d all data/%	4.12, 5.61	2.81, 5.30	5.56, 7.09
$\Delta\rho$ /e Å ⁻³	0.43, -0.42	0.67, -0.43	1.07, -0.86
CCDC entry	1470462	1470463	1470464

Table S1 continued

Compound	14	15·AcOEt
Formula	C ₁₁₀ H ₆₀ Ag ₂ B ₂ F ₄₈ Fe ₂ N ₂ P ₂	C ₅₀ H ₄₄ AgBF ₄ Fe ₂ N ₂ O ₂ P ₂
<i>M</i>	2732.60	1073.19
Crystal system	triclinic	orthorhombic
Space group	<i>P</i> -1 (no. 2)	<i>P</i> 2 ₁ 2 ₁ 2 ₁ (no. 19) ^d
<i>a</i> /Å	12.0872(3)	9.5212(3)
<i>b</i> /Å	14.0822(3)	21.6705(6)
<i>c</i> /Å	17.7896(4)	22.1659(7)
α /°	69.1784(7)	90
β /°	72.1205(7)	90
γ /°	83.0402(7)	90
<i>V</i> /Å ³	2693.4(1)	4573.5(2)
<i>Z</i>	1	4
μ (Mo K α)/mm ⁻¹	0.785	1.179
Diffns collected	41341	40999
Independent diffns	12377	10500
Observed ^c diffns	10921	9875
<i>R</i> _{int} ^d /%	1.98	3.09
No. of parameters	757	607
<i>R</i> ^d obsd diffns/%	3.64	2.52
<i>R</i> , <i>wR</i> ^d all data/%	4.22, 9.88	2.84, 5.52
$\Delta\rho$ /e Å ⁻³	1.35, -0.78	0.42, -0.26
CCDC entry	1470465	1470466

^d Flack's enantiomorph parameter: -0.01(1).

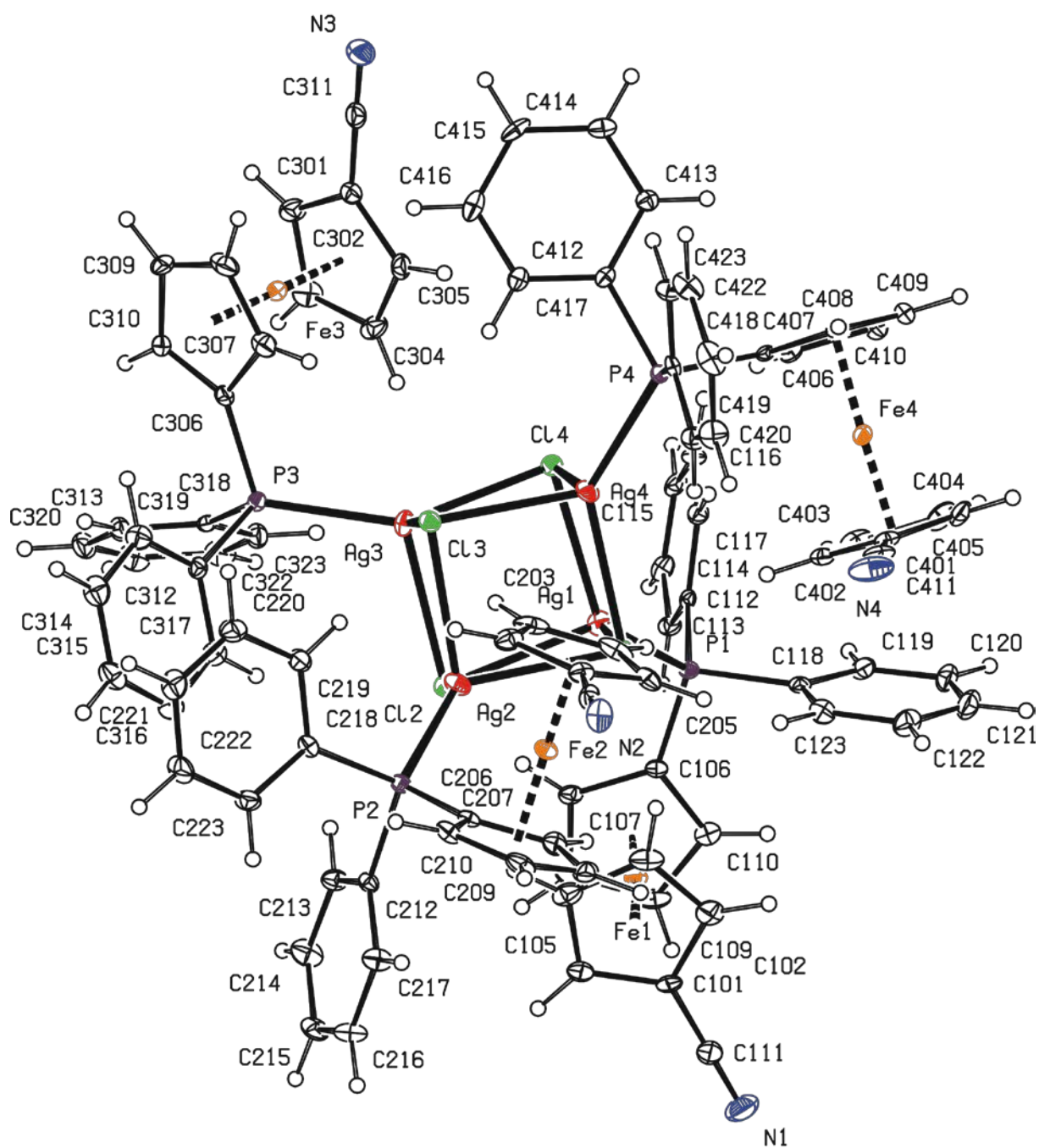


Figure S2. Complete view of the cubane molecule in the crystal structure of $2 \cdot \text{H}_2\text{O}$ showing displacement ellipsoids at the 30% probability level.

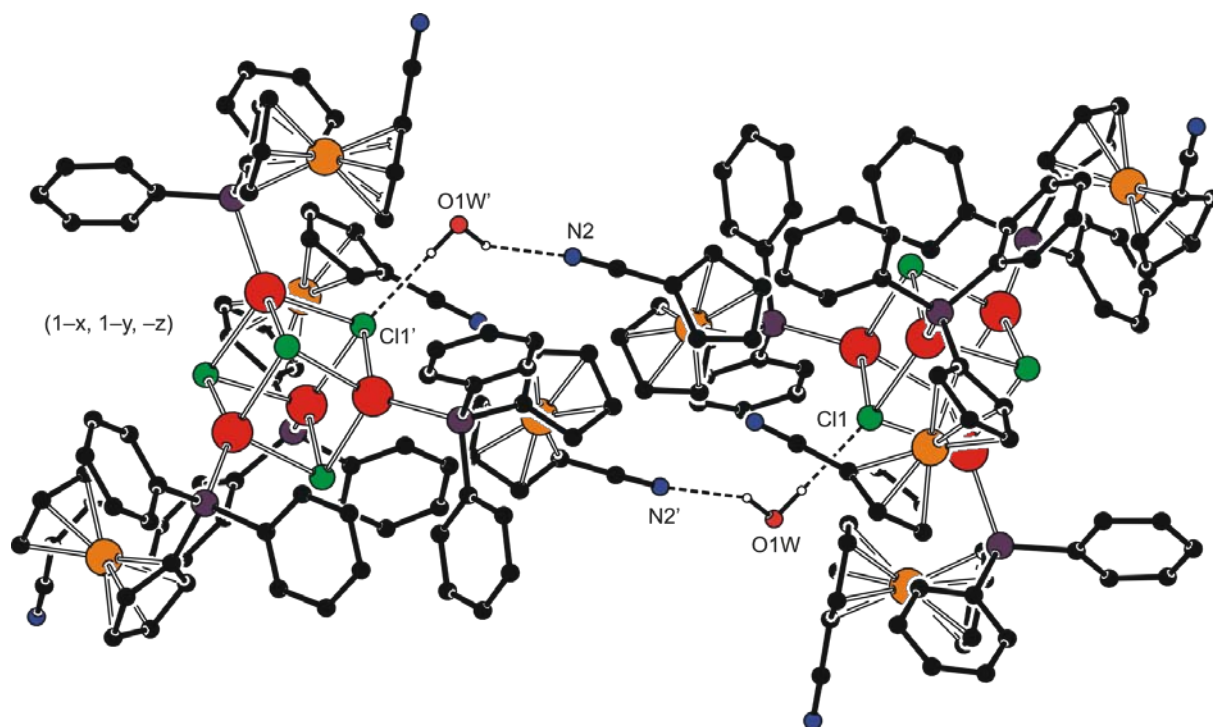


Figure S3. Hydrogen-bonding interactions in the structure of $2 \cdot \text{H}_2\text{O}$. H-bond parameters are as follows: $\text{O1W-H1W} \cdots \text{C11}$, $\text{O1W} \cdots \text{C11} = 3.348(3) \text{ \AA}$, angle at H1W = 161° ; $\text{O1W-H2W} \cdots \text{N2}^i$: $\text{O1} \cdots \text{N2}^i = 3.031(4) \text{ \AA}$, angle at H2W = 144° , i. $(1-x, 1-y, -z)$.

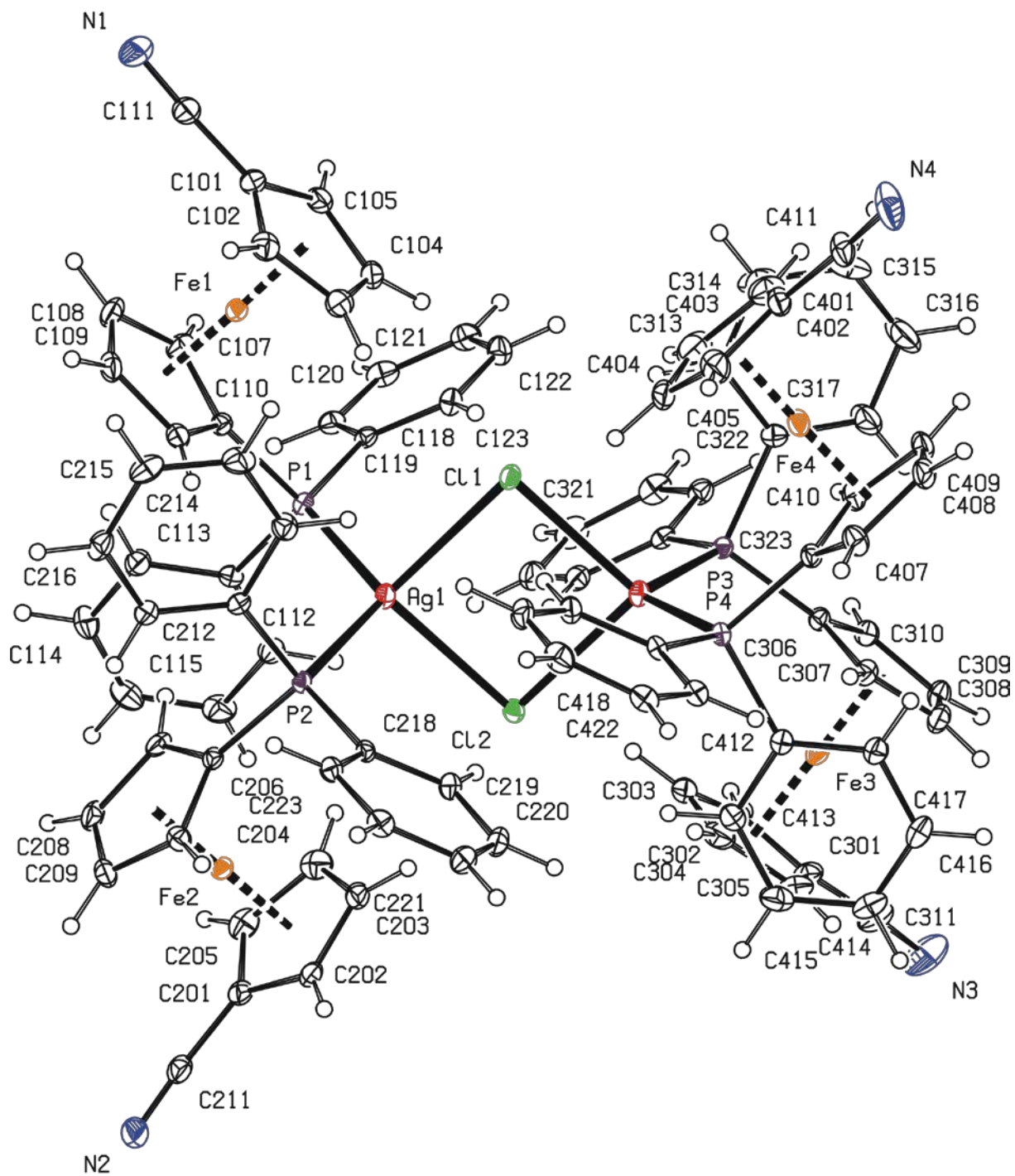


Figure S4. Complete view of the complex molecule in the crystal structure of **3**·CH₂Cl₂ showing displacement ellipsoids at the 30% probability level.

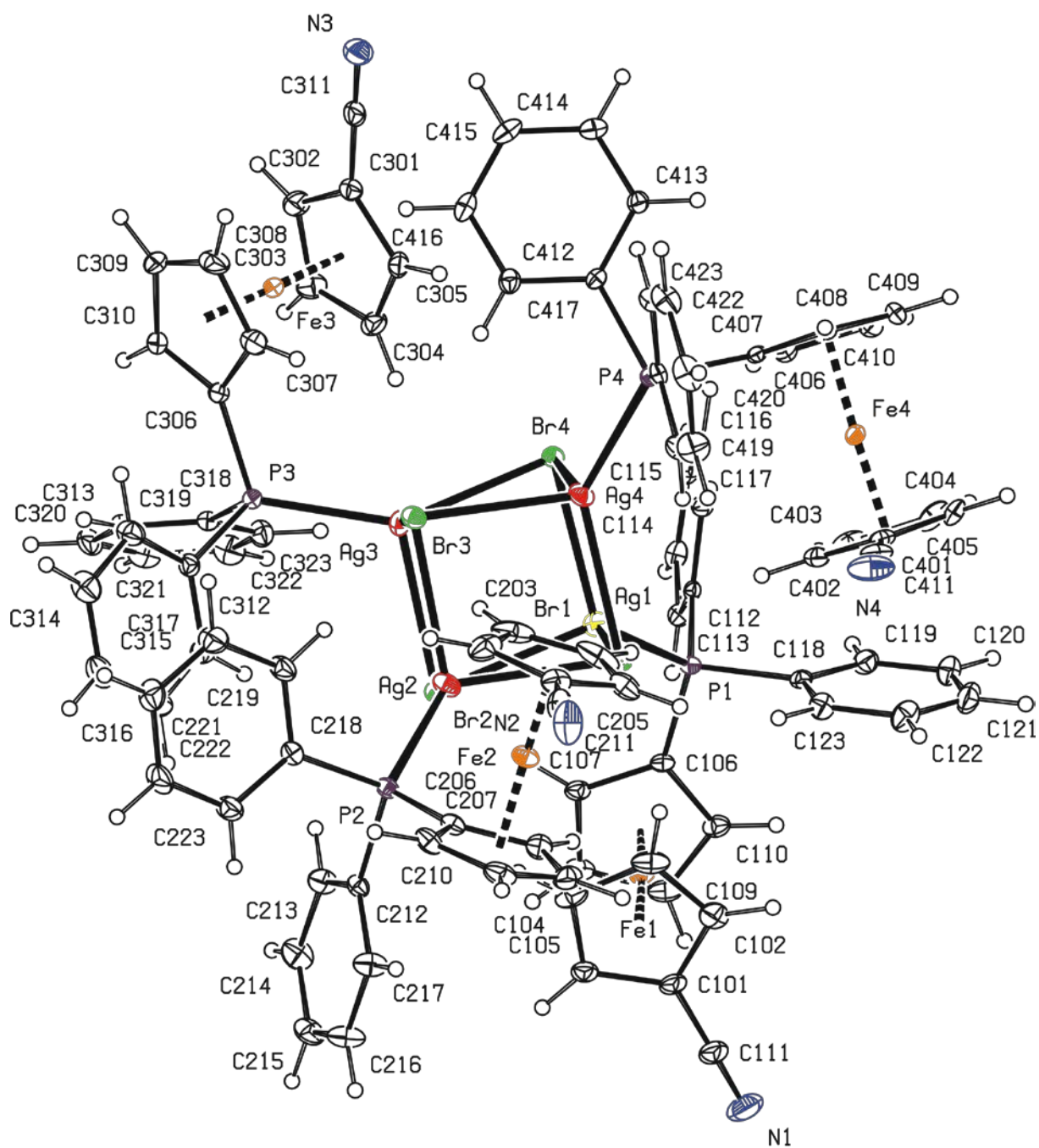


Figure S5. Complete view of the cubane molecule in the crystal structure of $4 \cdot 0.25\text{H}_2\text{O}$ showing displacement ellipsoids at the 30% probability level.

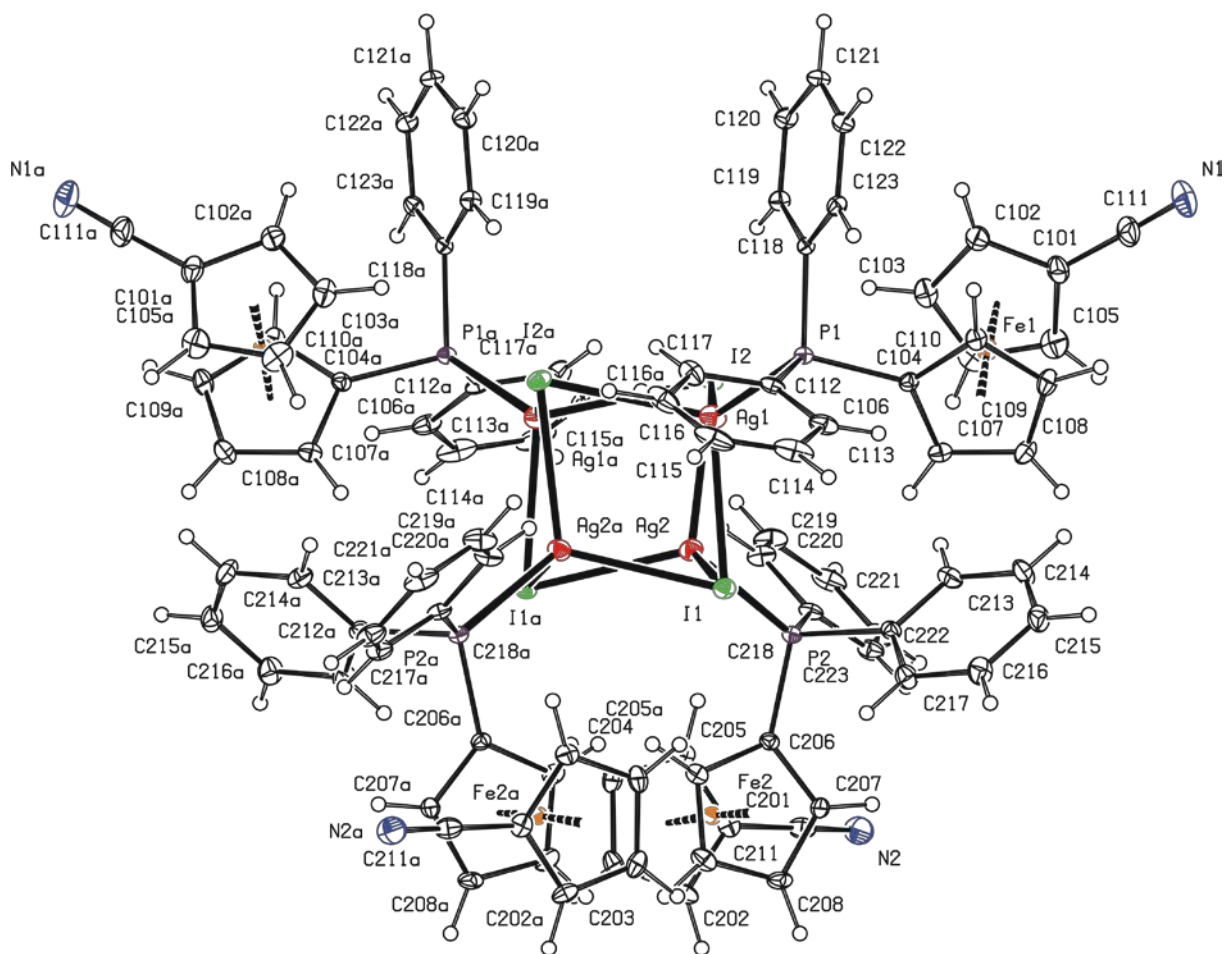


Figure S7. Complete view of the cubane molecule in the crystal structure of **5·4CHCl₃** showing displacement ellipsoids at the 30% probability level.

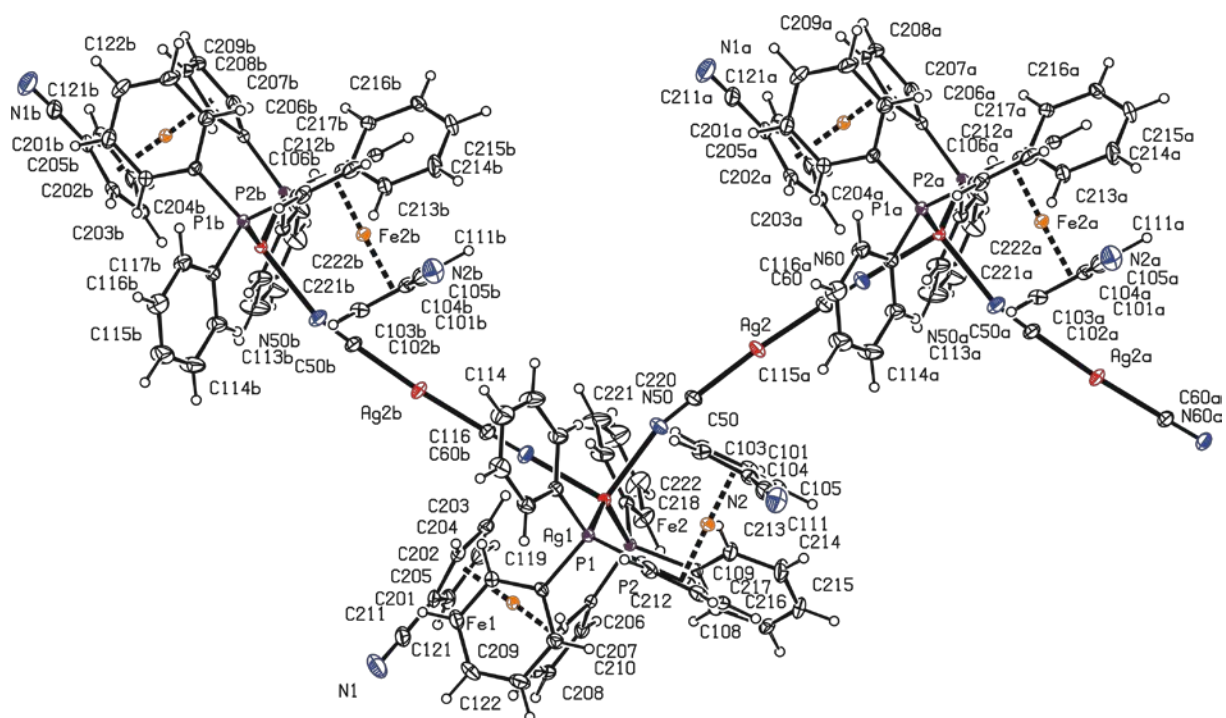


Figure S8. PLATON plot of the infinite chain in the structure of solvated **6** showing displacement ellipsoids at the 30% probability level.

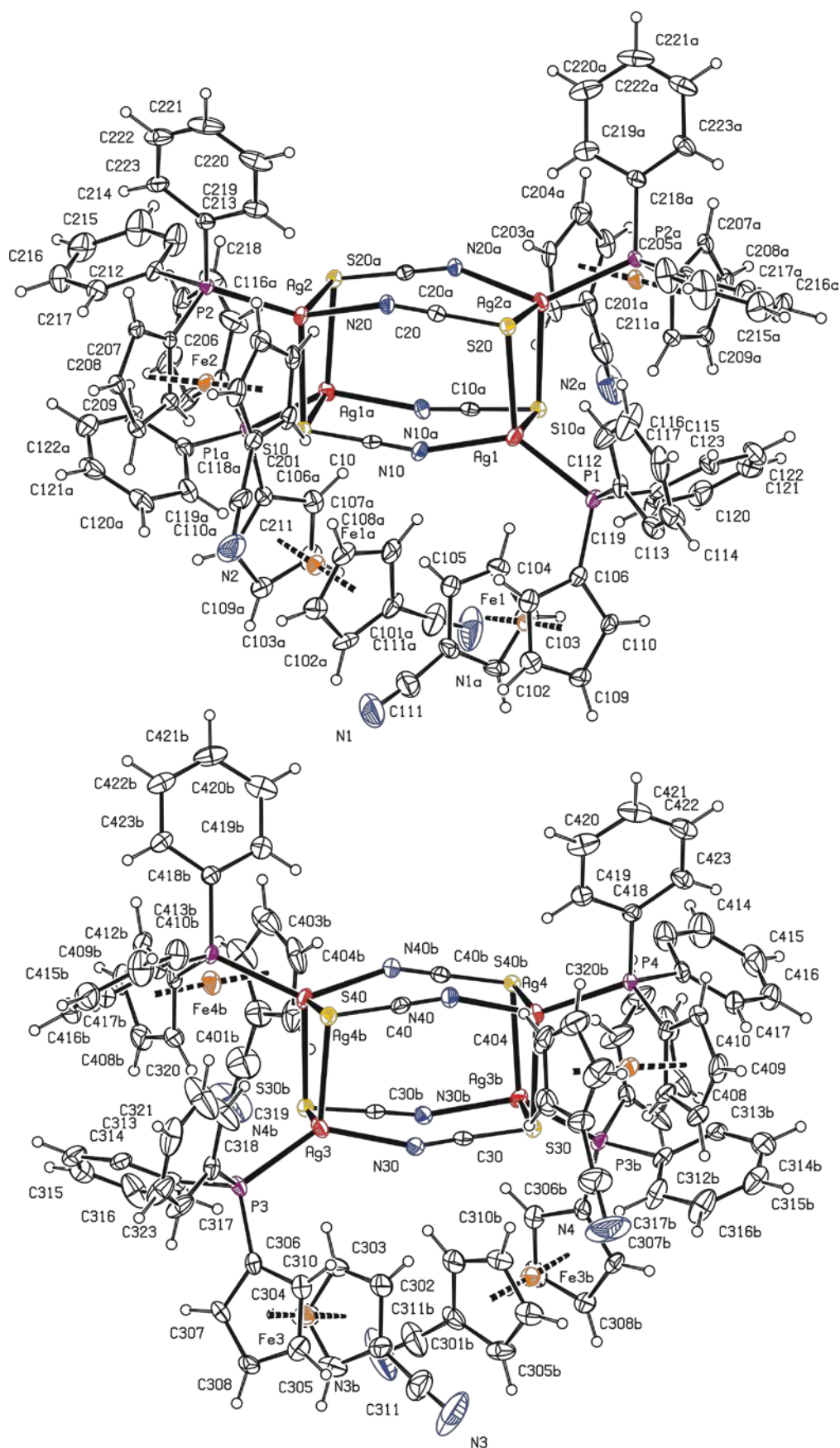
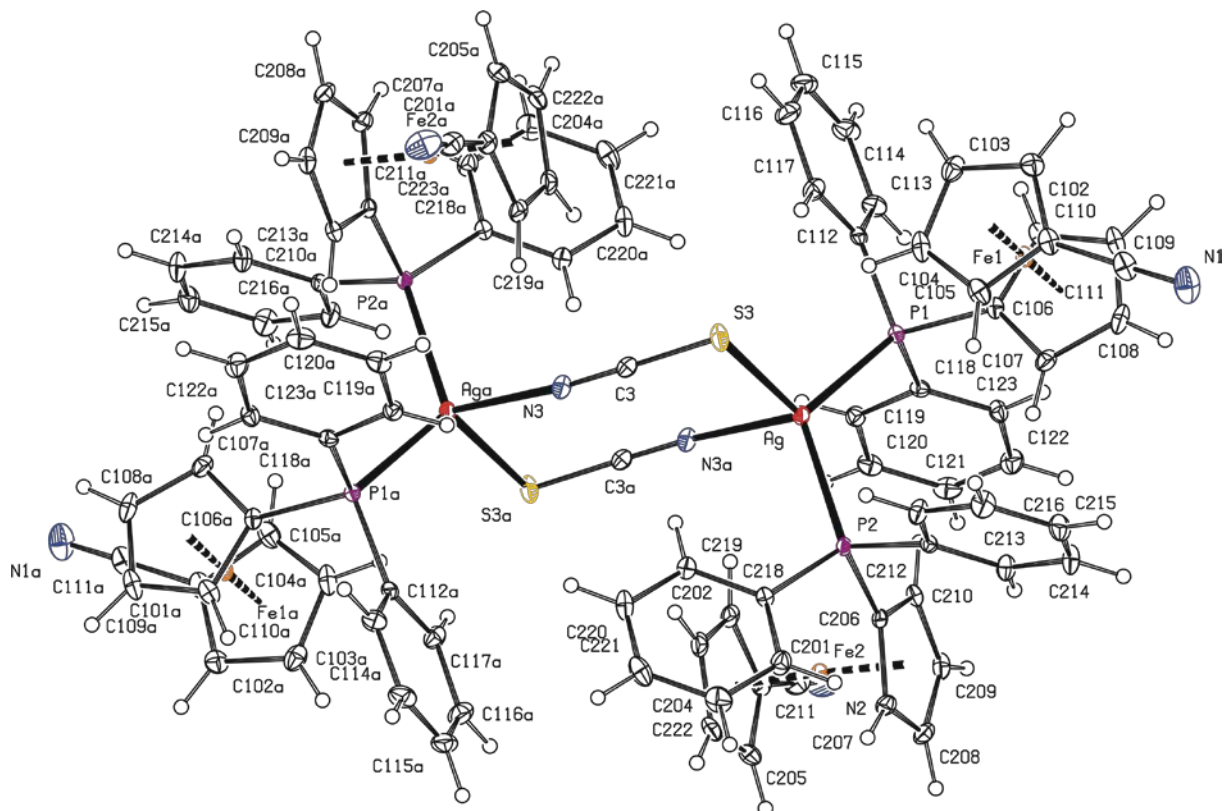


Figure S9. PLATON plot of the two the cubane molecules in the crystal structure of solvated **7** showing displacement ellipsoids at the 30% probability level.



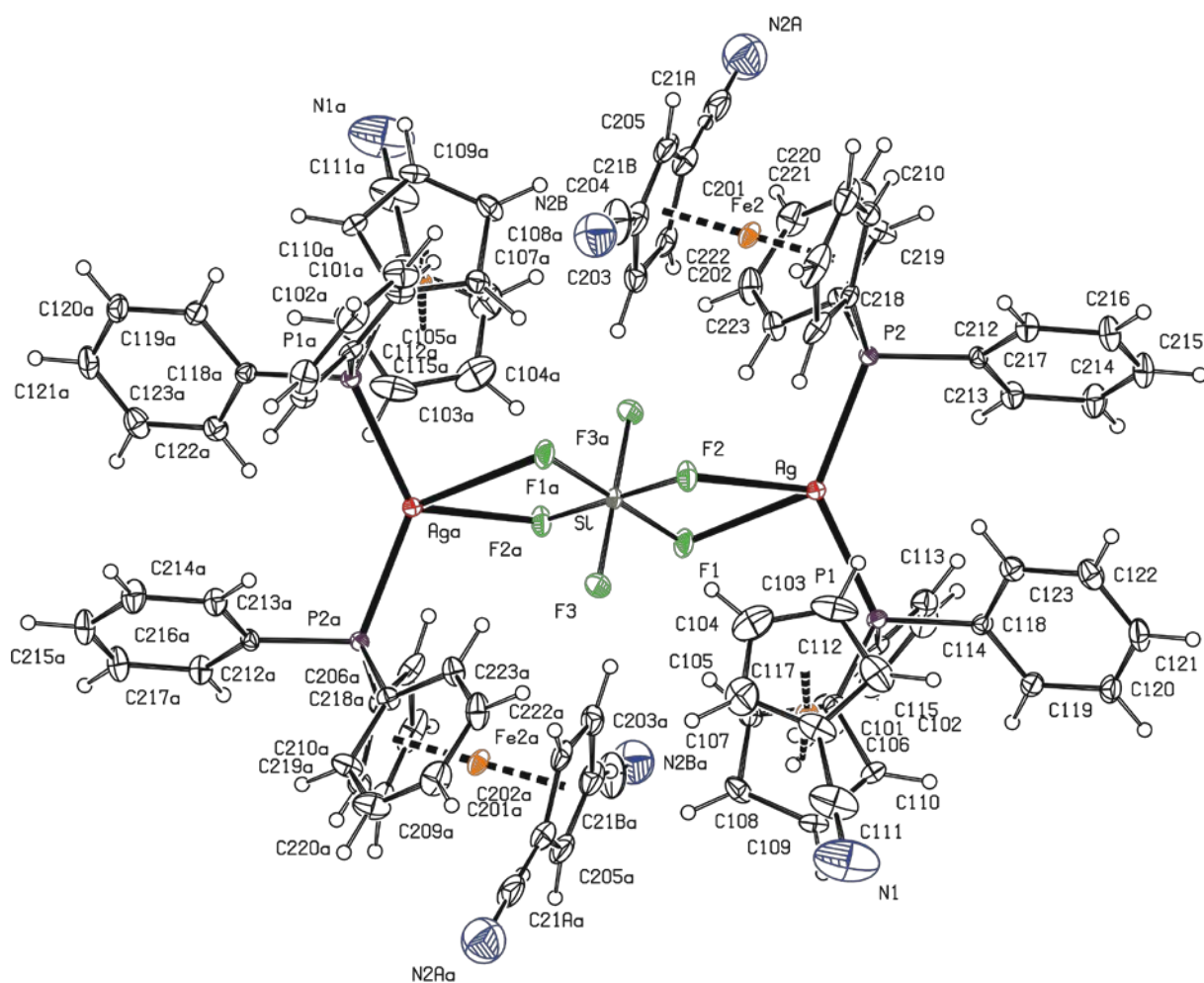


Figure S12. Complete view of the cubane molecule in the crystal structure of solvated **10** showing displacement ellipsoids at the 30% probability level and both positions of the disordered CN group.

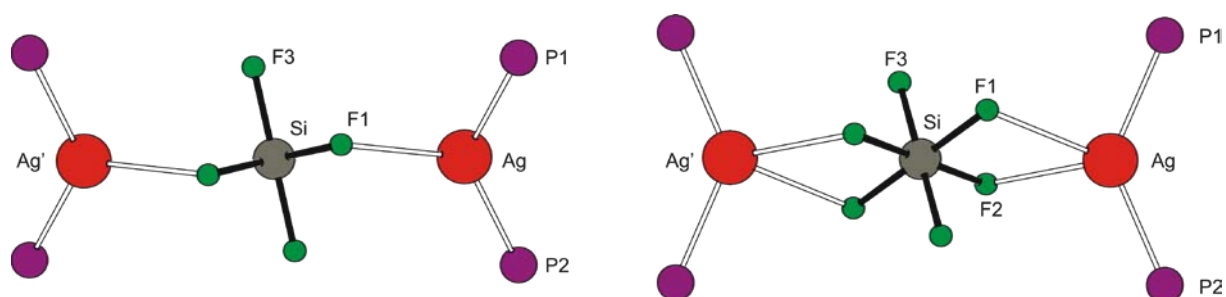


Figure S13. Alternative views of the $P_2Ag_2(SiF_6)$ core in **10**.

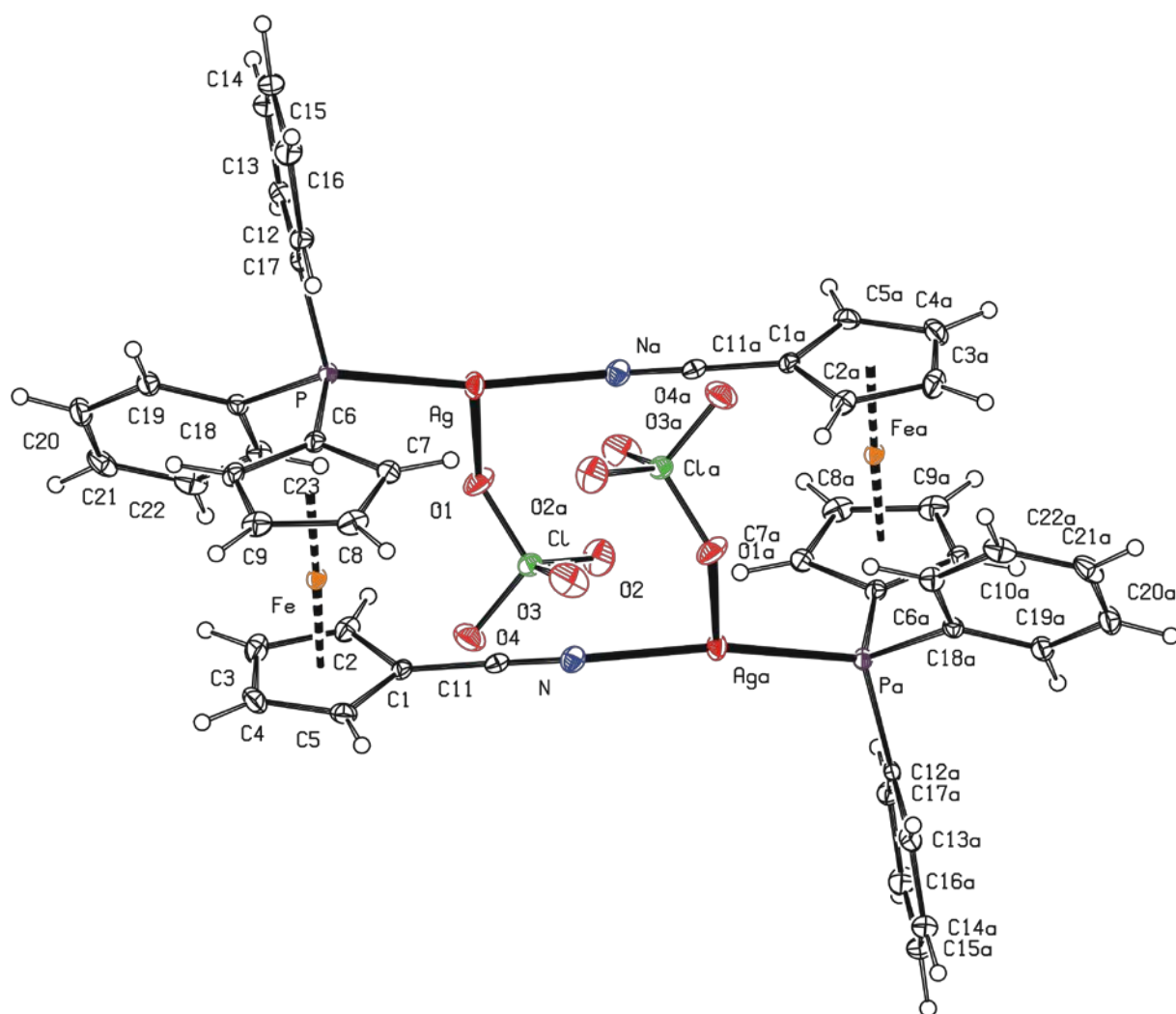


Figure S14. Complete view of the structure of **11** showing displacement ellipsoids at the 30% probability level.

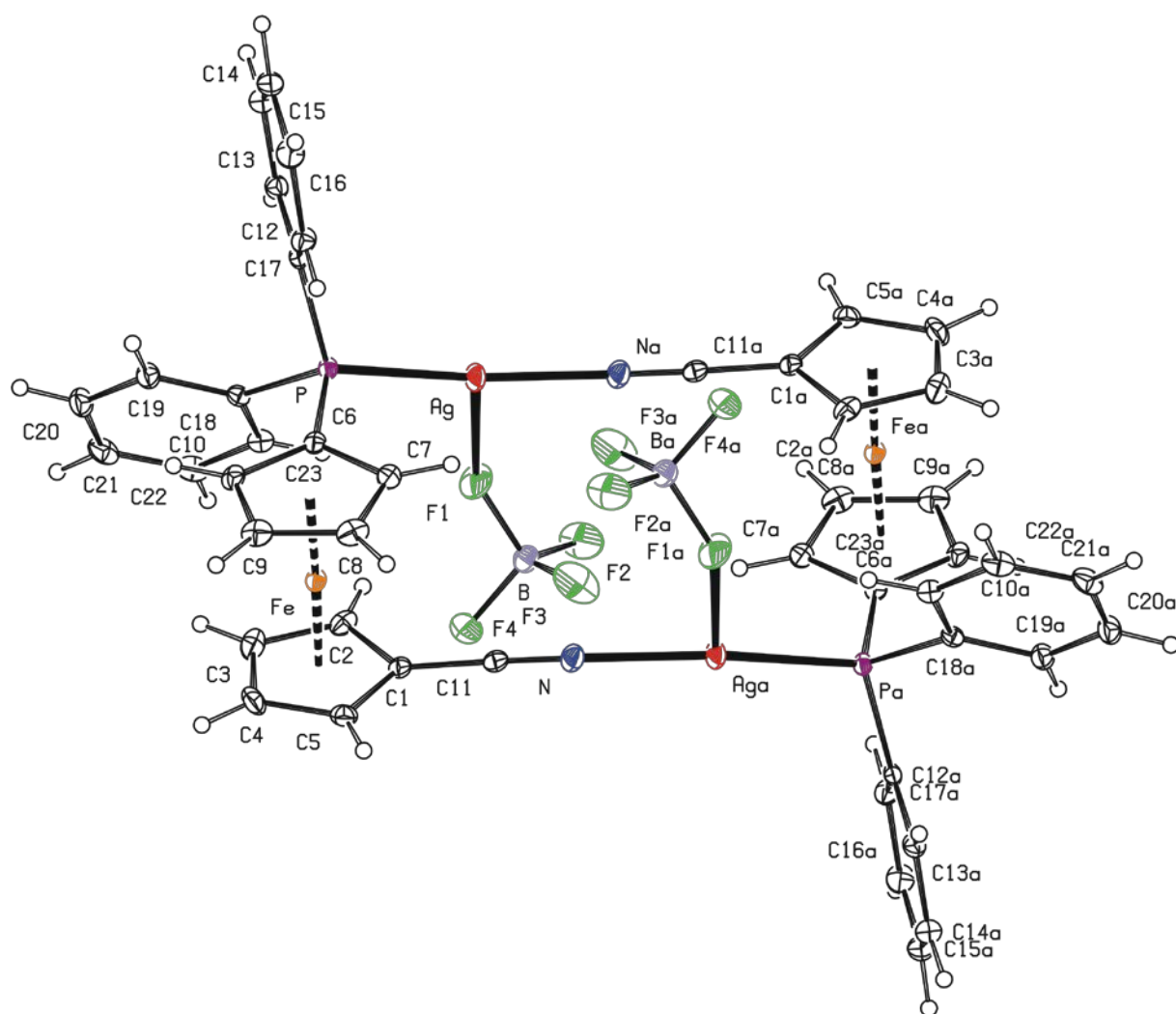


Figure S15. Complete view of the structure of **12** showing displacement ellipsoids at the 30% probability level.

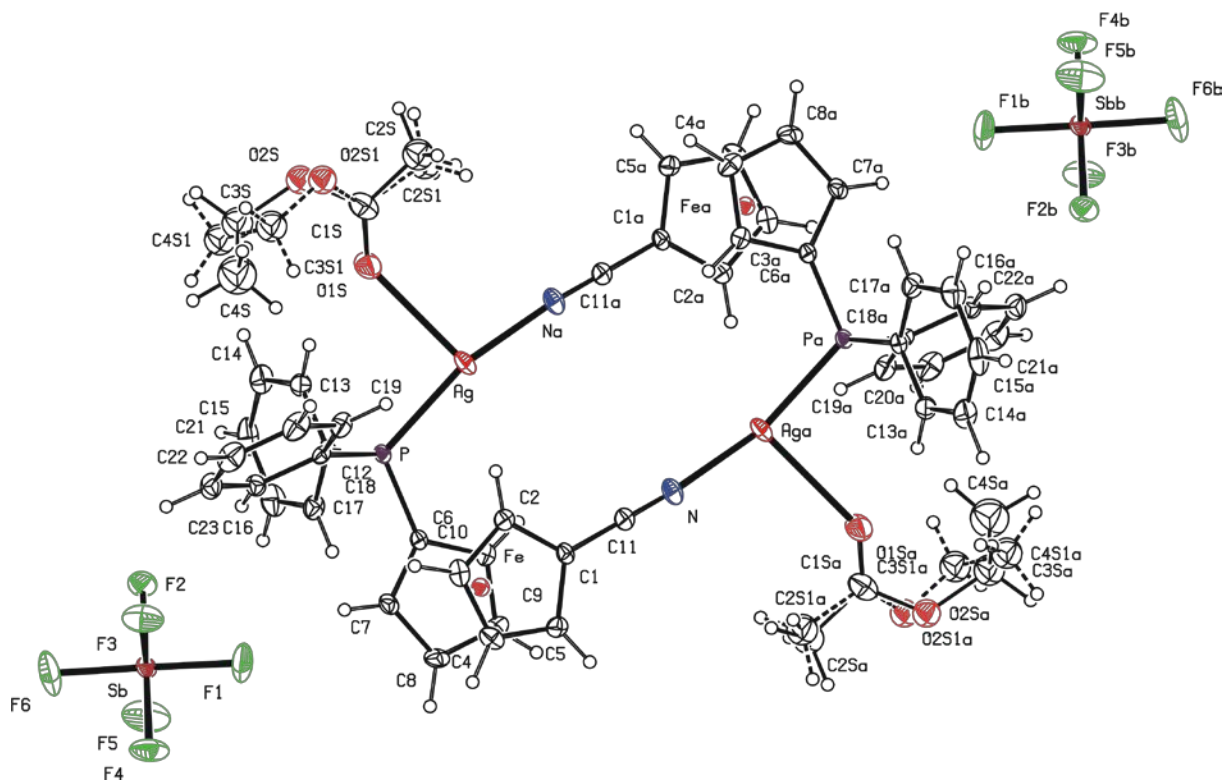


Figure S16. Complete view of the structure of **13** showing displacement ellipsoids at the 30% probability level.

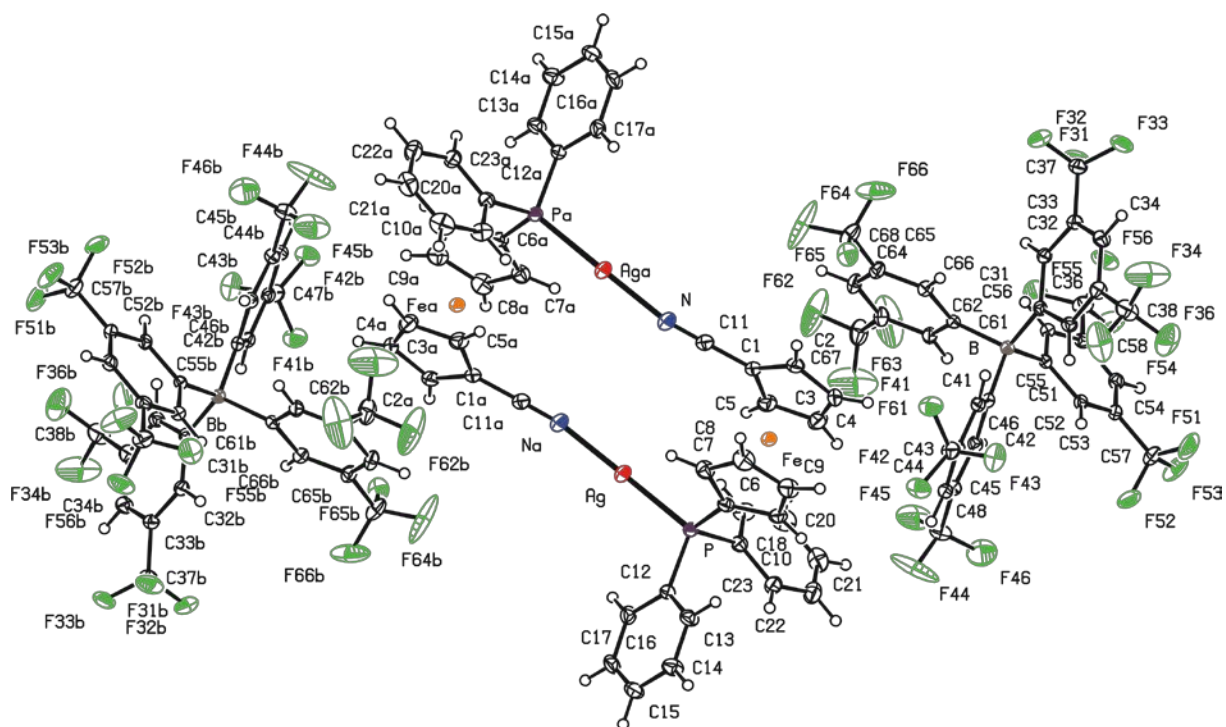


Figure S17. Complete view of the structure of **14** showing displacement ellipsoids at the 30% probability level.

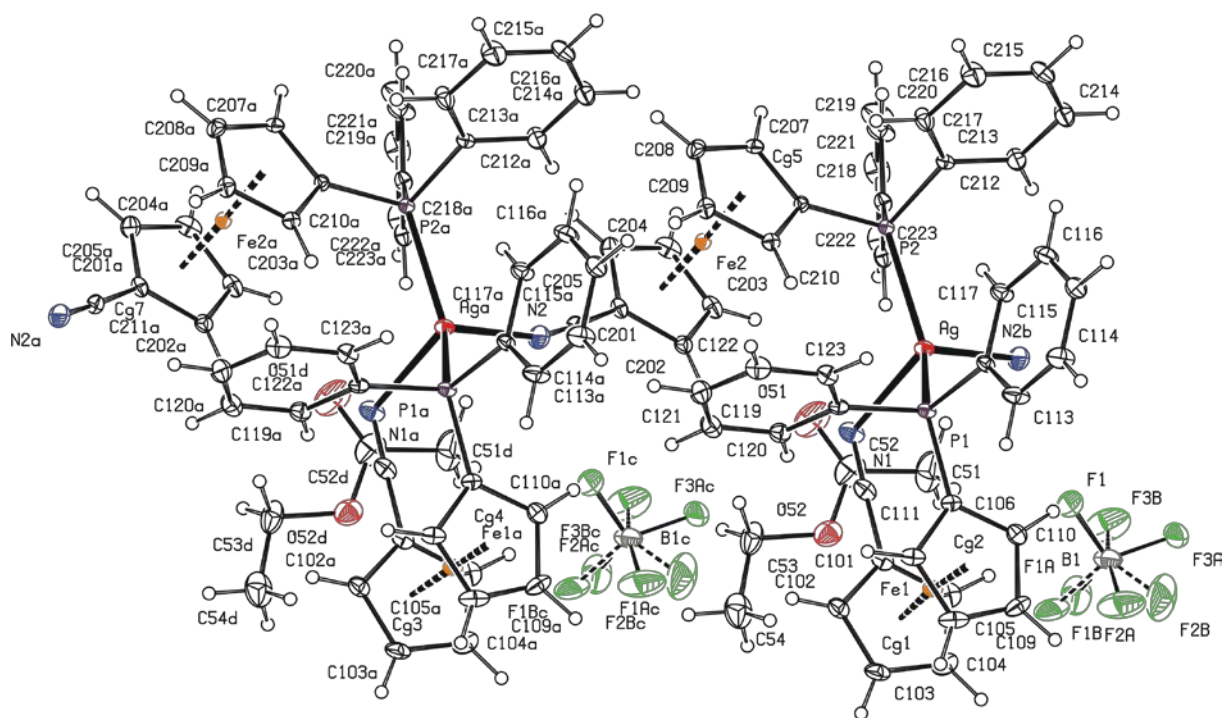


Figure S18. PLATON plot the polymeric structure of **15**·AcOEt. Displacement ellipsoids enclose the 30% probability level.

Table S2. Asymmetry factors Q for the individual faces of the heterocubane cores in **2**·H₂O, **4**·0.25H₂O, **5**·3AcOEt, and **5**·4CHCl₃.^a

Parameter	2 ·H ₂ O	4 ·0.25H ₂ O	Parameter	5 ·3AcOEt	5 ·4CHCl ₃
$Q_{1,2}$	0.995	0.958	$Q_{1,2}$	0.663	0.656
$Q_{1,3}$	0.908	0.851	$Q_{1,1'}$	0.842	0.804
$Q_{1,4}$	0.925	0.868	$Q_{1,2'}$	0.752	0.730
$Q_{2,3}$	0.835	0.791	$Q_{2,1'}$	≡ $Q_{1,2'}$	≡ $Q_{1,2'}$
$Q_{2,4}$	0.980	0.915	$Q_{2,2'}$	0.746	0.697
$Q_{3,4}$	0.994	0.942	$Q_{1',2'}$	≡ $Q_{1,2}$	≡ $Q_{1,2}$

^a Parameter $Q_{i,j}$ is defined as the ratio of the diagonal Ag···Ag and X···X distances on the face containing atoms Ag_i and Ag_j ($Ag···Ag/X···X$; *N.B.* the halogen atoms need not have the same numbers as the silver atoms $Ag_{i,j}$).

DFT computations. All calculations were performed using the density-functional theory (DFT) Becke's three-parameter functional⁹ using the non-local Lee-Yang-Parr correlation functional (B3LYP)¹⁰ with the standard 6-31G* basis set for all atoms except for Ag, where D95 basis set¹¹ with effective core potential¹² was used, as implemented in the Gaussian 09 program package.¹³ Geometry optimizations started from the experimentally determined solid-state structures using analytically constructed gradients. The starting geometries for the model species **F** and **G** were taken as fragments of the structures of (1,2,3,4,5-pentacyanocyclopentadienide- κN)tris(triphenylphosphine)silver(I)¹⁴ and **15**, respectively. At the stationary points, natural population analysis¹⁵ was carried out and electron density and its Laplacian were plotted. Optimized coordinates of all calculated structures are given in the Supporting Information.

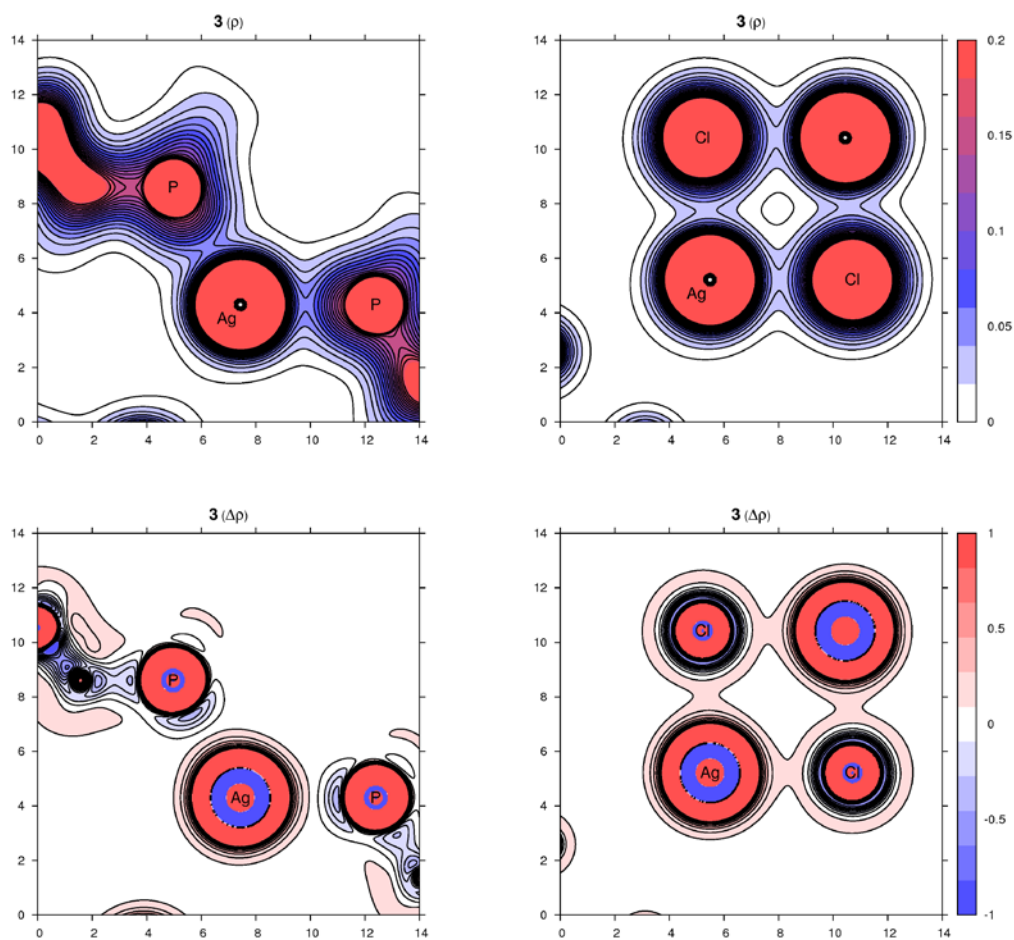


Figure S19. Additional contour plots of the electron density $\rho(r)$ (top panel) and its Laplacian $\Delta\rho(r)$ (bottom panel) for compound **3** in plane defined by three atoms whose symbols are indicated in the Figure. All values are in atomic units.

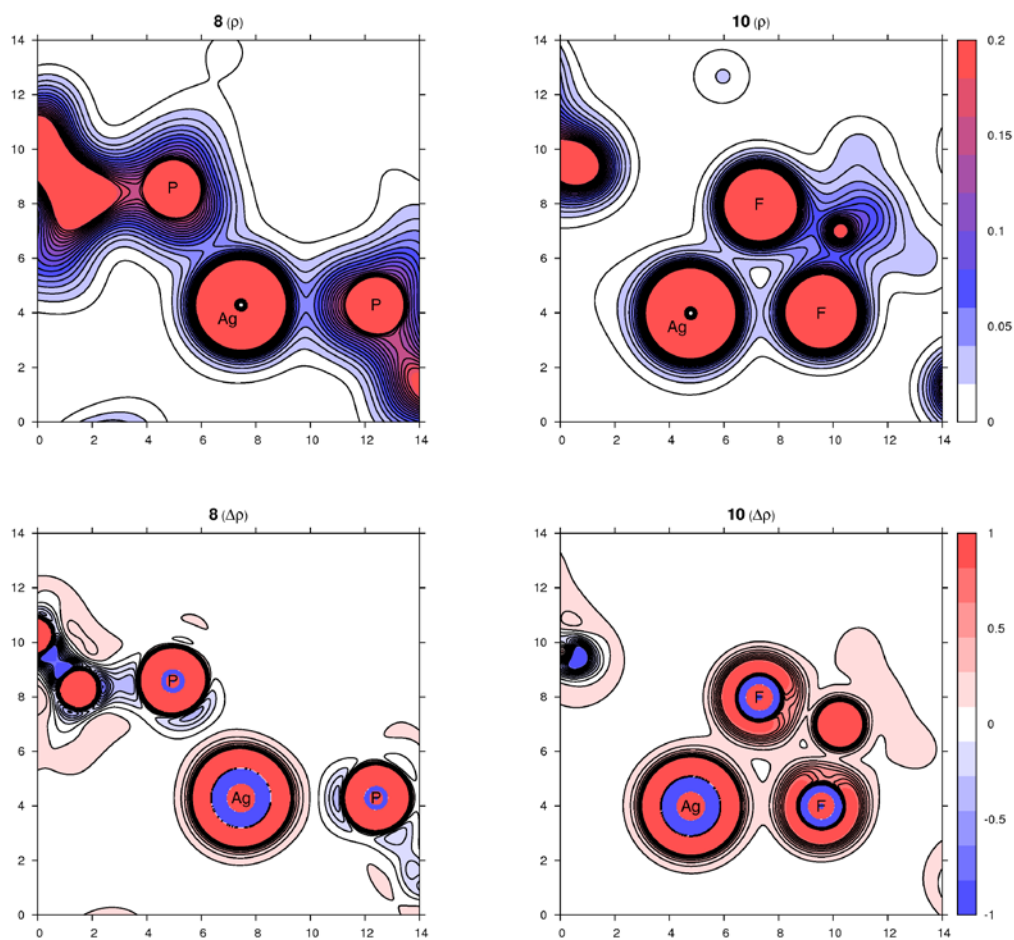


Figure S20. Contour plots of the electron density $\rho(r)$ (top panel) and its Laplacian $\Delta\rho(r)$ (bottom panel) for compounds **8** (left part) and **10** (right part) in plane defined by three atoms whose symbols are shown. All values are in atomic units.

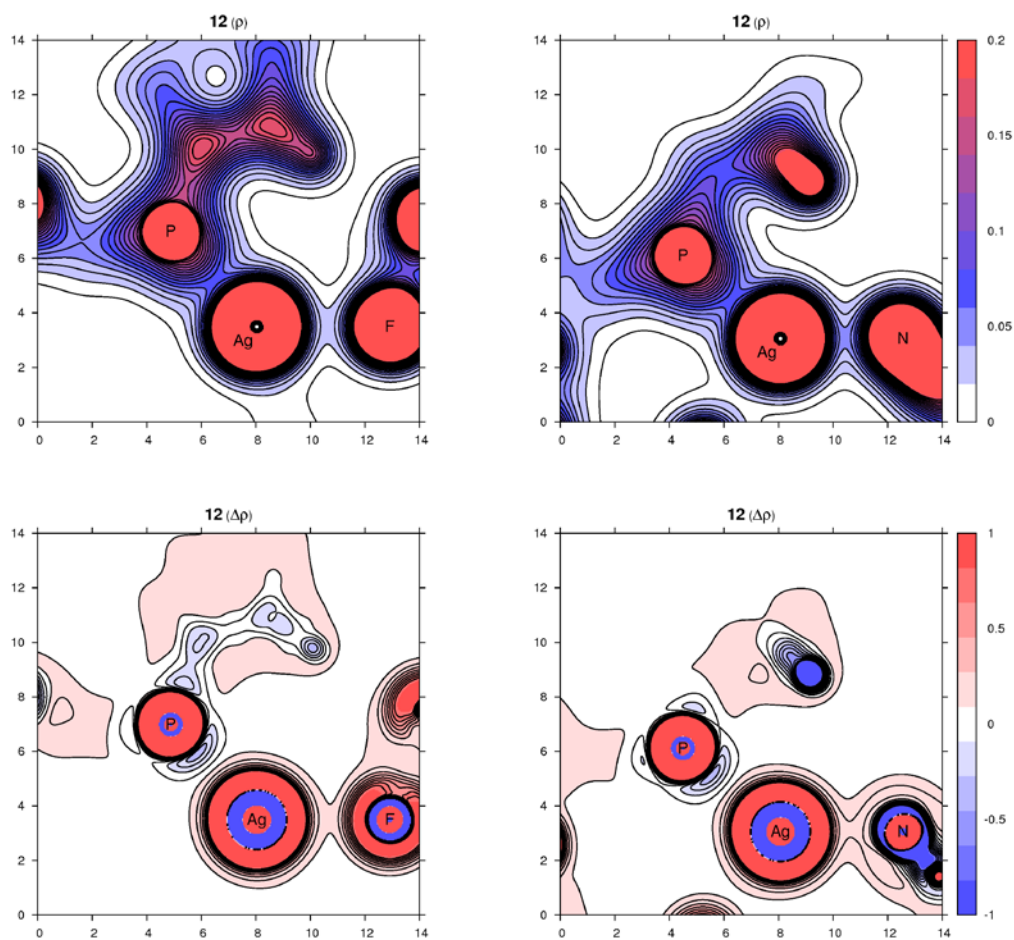


Figure S21. Contour plots of the electron density $\rho(r)$ (top panel) and its Laplacian $\Delta\rho(r)$ (bottom panel) for compound **12** in planes defined by three atoms whose symbols are indicated. All values are in atomic units.

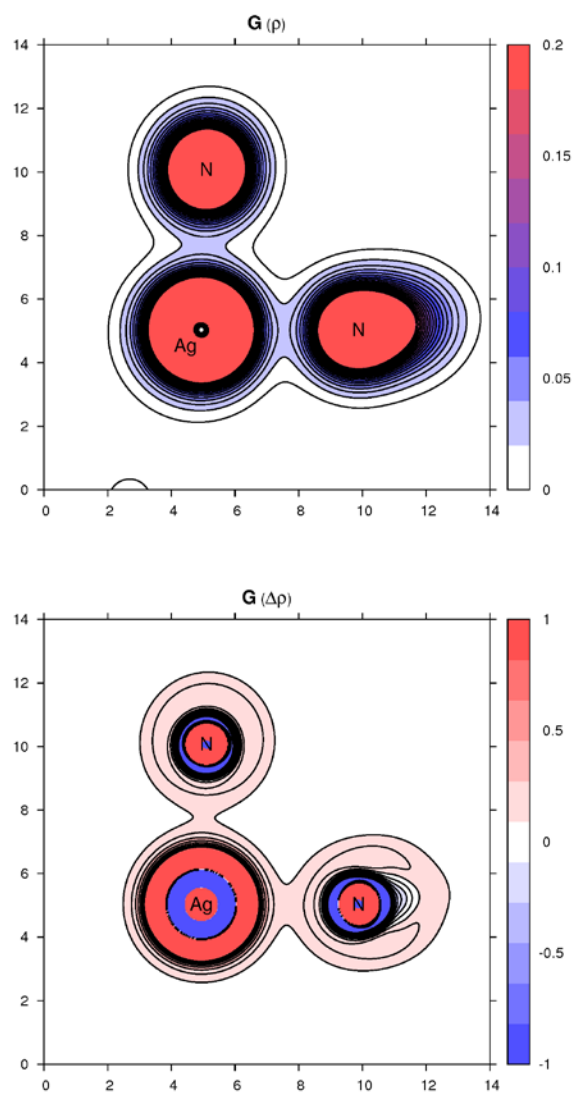


Figure S22. Contour plots of the electron density $\rho(r)$ (top panel) and its Laplacian $\Delta\rho(r)$ (bottom panel) for the model species **G** in the plane defined by Ag and its bonding nitrogen atoms. All values are in atomic units.

References

1. Škoch, K.; Císařová, I.; Štěpnička, P. *Inorg. Chem.* **2014**, *53*, 568-577.
2. Padma, D. K. *Synth. React. Inorg. Met.-Org. Chem.* **1988**, *18*, 401-404.
3. Zhang, Y.; Santos, A. M.; Herdtweck, E.; Mink, J.; Kühn, F. E. *New J. Chem.* **2005**, *29*, 366-370.
4. The assignment of the IR bands is based on the comparison with the literature: a) Silverstein, R. M.; Webster, F. X.; Kiemle, D. J. *Spectrometric Identification of Organic Compounds*, 7th ed.; Wiley, New York, 2005; b) Nakamoto, K. *Infrared and Raman Spectra of Inorganic and Coordination Compounds*, 5th ed.; Wiley, New York, 1997.
5. Sheldrick, G. M. *Acta Crystallogr., Sect. A: Fundam. Crystallogr.* **2008**, *64*, 112-122.
6. Sheldrick, G. M. *Acta Crystallogr., Sect. C: Struct. Chem.* **2015**, *71*, 3-8.
7. Spek, A. L. *Acta Crystallogr., Sect. C: Struct. Chem.* **2015**, *71*, 9-18.
8. Spek, A. L. *J. Appl. Crystallogr.* **2003**, *36*, 7-13.
9. Becke, A. D. *J. Chem. Phys.* **1993**, *98*, 5648-5652.
10. Lee, C.; Yang, W.; Parr, R. G. *Phys. Rev. B: Condens. Matter* **1988**, *37*, 785-789.
11. Dunning Jr., T. H.; Hay, P. J. in *Modern Theoretical Chemistry*, Ed. H. F. Schaefer III, Vol. 3, pp.1-28; Plenum Press, New York, 1977.
12. Hay, P. J.; Wadt, W. R. *J. Chem. Phys.* **1985**, *82*, 270-283.
13. Gaussian 09, Revision E.01, Gaussian, Inc, Wallingford CT, 2010.
14. Less, R. J.; Guan, B.; Muresan, N. M.; McPartlin, M.; Reisner, E.; Wilson, T. C.; Wright, D. S. *Dalton Trans.* **2012**, *41*, 5919-5924.
15. Foster, J. P.; Weinhold, F. *J. Am. Chem. Soc.* **1980**, *102*, 7211-7218.